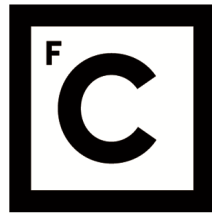


UNIVERSIDADE DE LISBOA  
FACULDADE DE CIÊNCIAS  
DEPARTAMENTO BIOLOGIA ANIMAL



**Ciências  
ULisboa**

**How *Lama2*-deficiency impacts myoblast differentiation in a mouse model for LAMA2-congenital muscular dystrophy**

Vanessa Filipa Laranjeiro Ribeiro

**Mestrado em Biologia Evolutiva e do Desenvolvimento**

Dissertação orientada por:  
Professora Doutora Sólveig Thorsteinsdottir e Doutora Ana Rita Carlos

## Index

Index .....	II
Acknowledgements .....	IV
Abstract.....	V
Resumo alargado .....	VI
List of Figures and Tables .....	VIII
List of abbreviations and symbols.....	IX
1. Introduction .....	1
1.1 Laminin's role in the extracellular matrix (ECM).....	1
1.2 Myogenesis.....	4
1.3 Essential players in skeletal muscle formation.....	5
1.3.1 Nfix.....	5
1.3.2 Myostatin.....	6
1.3.3 Jak-Stat .....	7
1.3.4 FAK .....	7
1.4 ECM mutations and muscular dystrophy .....	8
1.5 ECM mutations and Cancer.....	9
1.6 Aims of the project .....	10
2. Material and Methods.....	11
2.1 Mice and fetus collection.....	11
2.1.1 Genotyping .....	11
2.2. <i>In Vitro</i> approach.....	11
2.2.1. C2C12 cell line .....	11
2.2.2 Cancer cell lines .....	11
2.2.3 Cell Culture .....	12
2.2.4 Differentiation assay.....	12
2.3 Real Time-qPCR .....	12
2.3.1 RNA extraction.....	12
2.3.2 cDNA and RT-qPCR.....	12
2.4 Western Blot.....	13
2.4.1 Protein extraction.....	13
2.4.2 Western Blot.....	13
2.5. Immunofluorescence .....	14
2.5.1 Cell lines .....	14
3. Results .....	15
<i>Lama2</i> -deficiency alters the <i>myogenin</i> pathway in C2C12 cells, and to a lesser extent <i>in vivo</i> . .....	15
<i>Lama2</i> -deficiency alters Nfix expression and Myf5 localization in C2C12 cells.....	16
Effect of <i>Lama2</i> -deficiency on RhoA and Erk pathways in C2C12 cells .....	20
Effect of <i>Lama2</i> -deficiency on <i>Akirin1</i> and <i>Notch1</i> expression.....	21
<i>Lama2</i> -deficiency impacts myoblasts differentiation of C2C12 cells in vitro.....	22

Jak-Stat3 pathway is altered in the context of <i>Lama2</i> -deficiency in C2C12 cells, and to a lesser extent <i>in vivo</i> .....	24
<i>Lama2</i> -deficiency impacts FAK signaling pathway <i>in vitro</i> and <i>in vivo</i> .....	25
Impact of <i>LAMA2</i> absence in cancer cells.....	26
4. Discussion.....	28
Annex .....	33
Bibliography .....	36

## Acknowledgements

This was a year full of challenges and a great learning journey.

First, I would like to thank the two people that allowed this incredible experience to happen, my supervisors, Sólveig Thorsteinsdóttir and Ana Rita Carlos. In the most difficult period of my life, I will never forget the words, affection, and strength that you both had to me. Sólveig thank you so much for always listening, encouraging, and teaching me so much, it is a pleasure to work with you. Rita is a pleasure to have you as my supervisor, to learn with you every day, you are such an inspiration. All the challenges with you seem less difficult, and you encourage us to always believe that we can do it and we are able to be the best. I want to thank you for all the affection, for the support in the most difficult times and mainly for believing in me.

Second, I would like to thank Susana Martins for all the care and patience that you had with me during this project teaching me all the techniques and experiments, you were tireless. It was a year with a lot of work, but very funny moments as well, and I'm very grateful to had the opportunity to learn and work with you. Thank you for always being there for me and encouraging me to always give my best. I also want to thank you and Catarina Melo for the time you spent helping me with the reviewing the thesis and all the moments we had together as *Las chicas cantantes*, making our days cheerful.

Then, I would like to thank to Marta Palma for all the lab support, and to Joaquim Tapisso for the help in the animal house.

I also want to thank Gabriela Rodrigues and Rita Zilhão for all the comments and discussions, I learned a lot with you, Luis for all the support in microscopy, Inês Fonseca, Ana Rita Soares, Hugo Luiz, Pedro Santos, and Antonio Cordero for sharing experiences and funny moments in the lab and lunch times, making the days a bit lighter. I also want to highlight how important, and fun were the group walks every Wednesday, it was a great team building activity.

For their contribution to the thesis presented here, I also would like to thank Susana Martins for the help in validating all the *in vivo* data and Hugo Luiz for the dedication and help in characterizing the colorectal cancer cell lines.

I want to thank the support given to this project by Association Française contre le Myopathies (AFM) Téléthon (contract no. 23049), L'Oréal Portugal Medals of Honor for Women in Science 2019, and Fundação para a Ciência e Tecnologia Project (Ref. PTDC/BTM-ORG/1383/2020) and Unit Funding (Ref. UIDB/00329/2020). I also want to thank the generosity of our donor Henrique Meirelles who chose to support the MATRIHEALTH Project.

Last, but not least, I would like to thank my family and friends. To my parents, a special thank for the effort and support in this difficult period of my life, to always being there for me and for not letting me give up. To my friends, for all the motivation, for believing and always being there for me and for making my life lighter.

## Abstract

Extracellular matrices (ECMs) play a critical biochemical and structural role for cells and tissues. Their biochemical role is, for example, acting as a vehicle and reservoir for multiple factors, and their structural roles, help stabilize cells and tissues providing a solid-phase cell adhesion substrate. Mutations in ECM components can lead to the development of muscular dystrophies. Whether mutations in these components can impact other diseases, particularly, cancer, requires further studies. *LAMA2*-congenital muscular dystrophy (LAMA2-CMD) is a neuromuscular disease triggered by mutations in *LAMA2*, codifying the  $\alpha 2$  chain of laminins 211/221, a structural component of basement membranes. Basement membranes are a specific type of ECM that is in direct contact with cells. When laminins 211/211 are absent, skeletal muscles display reduced muscle strength and failed muscle regeneration. Using the *dy<sup>w</sup>* mouse model for LAMA2-CMD, previous studies from the host laboratory indicated that laminin 211 may play an important role during normal muscle development and growth. Specifically, between embryonic day (E)17.5 and E18.5, the number of Pax7- and myogenin-positive cells becomes reduced in *dy<sup>w</sup>* fetuses compared to controls and their muscle growth lags behind. Here a C2C12 myoblast cell line lacking *Lama2* was used to establish an *in vitro* model for LAMA2-CMD. This cell line was characterized by an impairment in myofiber formation when compared to the wildtype. With the aim of dissecting out how *Lama2* affects myoblast differentiation, this project focused on studying the Nfix pathway, known to be responsible for the switch between embryonic and fetal myogenesis, and the myogenin pathway, which leads to terminal myoblast differentiation. Additionally, other important pathways that impact differentiation, namely Jak-Stat, RhoA-Erk and FAK were also analyzed. mRNA and protein expression levels of these factors and some of their targets were validated *in vitro* and *in vivo*. The data obtained, particularly *in vitro*, suggests that *Lama2*-deficiency leads to a defect in myoblast differentiation. This is supported by 1) a significant increase in the levels of *Nfix* and a decrease in *Myog* expression, encoding myogenin, as well as a deregulation of their downstream targets; 2) a significant retention of Myf5 protein in the cytoplasm; and 3) a significant increase in P-Stat3. The increase in P-Stat3 was also observed in *LAMA2*-deficient cancer cell lines, suggesting that an increase in P-Stat3 may be a key consequence of *LAMA2* mutations, regardless of the type of disease. In summary, identifying the pathways and mechanisms deregulated in the absence of *LAMA2* is essential for the development of therapies that target disease onset directly.

**Keywords:** *Lama2*, LAMA2-CMD, ECM, Differentiation, Nfix.

## Resumo alargado

A matriz extracelular (MEC) é uma complexa rede acelular presente em todos os tecidos e fornece um suporte físico para as células. Embora a sua composição seja variável e específica dependendo do tecido, os principais constituintes são água, glicoproteínas (como colagénios, fibronectina e laminina), elastina, proteoglicanos e hialurano, que conjuntamente com outros componentes se designam de matrissoma. Existem dois tipos principais de MEC, a matriz intersticial de estrutura fibrosa ou semelhante a gel e a membrana basal que está em contacto com as células. A MEC tem a função de estabilização de células e tecidos, fornecendo substratos de adesão celular em fase sólida e ligando a MEC ao citoesqueleto das células via recetores transmembranares. A MEC desempenha também um papel chave como reservatório de fatores de crescimento e moléculas bioativas que controlam os comportamentos e características fundamentais das células como sinalização, proliferação, adesão, migração, polaridade, diferenciação e apoptose. Mutações nos componentes da MEC, nas proteínas transmembranares ou em proteínas que liguem a MEC ao citoesqueleto das células musculares esqueléticas podem levar a distrofias musculares. As distrofias musculares congénitas representam um grupo de doenças que causam fraqueza (hipotonia) e atrofia muscular, sendo detetadas logo, ou pouco após a nascença. Estas são doenças geralmente hereditárias e associadas a mutações autossómicas recessivas. A distrofia muscular associada ao gene *LAMA2* (LAMA2-CMD) é a distrofia muscular congénita mais comum e esta doença neuromuscular, tal como o nome indica, é desencadeada por mutações no gene *LAMA2*, que codifica para a cadeia  $\alpha 2$  das lamininas 211/221, levando à redução da força muscular e a constrangimentos na regeneração muscular, sendo que atualmente não existe cura para esta doença. A ausência desta proteína leva a danos nas miofibras e a tentativa de reparação deste dano por regeneração, através das células estaminais musculares adultas (células satélite), não ocorre com sucesso. As fibras musculares entram em degeneração através da indução de apoptose, que é seguida de regeneração e inflamação crónica, e como consequência o tecido muscular é substituído por tecido fibrótico e adipócitos. Estudos anteriores do laboratório utilizando a estirpe de ratinho *dy<sup>W</sup>*, a qual é um dos modelos mais utilizados para o estudo de LAMA2-CMD, sugerem que a laminina 211 desempenha um papel importante durante o desenvolvimento e crescimento muscular normais durante o período fetal. Em particular, os resultados mostraram que entre os dias embrionários (E)17.5 e E18.5, portanto durante o período fetal, o número de células musculares estaminais (células Pax7 positivas) e mioblastos diferenciados (células miogenina positivas) torna-se reduzido em fetos *dy<sup>W</sup>*, em comparação com os controlos e verifica-se um atraso no crescimento muscular. Contudo, desconhece-se que mecanismos causam esta redução no crescimento muscular, que vias de sinalização são afetadas e se a proliferação e/ou diferenciação das células estaminais musculares esqueléticas e mioblastos são afetadas.

Um dos objetivos deste projeto é compreender se a diferenciação de mioblastos está afetada na ausência de *Lama2*, e quais as vias envolvidas. Para tal foi utilizada uma linha celular de mioblastos, C2C12, na qual o gene *Lama2* se encontra mutado, com o objetivo de estabelecer um modelo *in vitro* para LAMA2-CMD que pudesse ser utilizado para responder a esta questão. A análise de células mutadas para *Lama2* permitiu revelar que a formação de miotubos fica comprometida nesta linha celular em comparação com a linha celular selvagem. Tendo feito esta observação, fulcral para o projeto, seguiu-se então o estudo de quais as vias responsáveis pelo defeito na diferenciação. Conhecida por ser responsável pela transição entre a miogénese embrionária e fetal, a via do Nfix foi um dos focos da análise das vias que afetam a diferenciação dos mioblastos, assim como a via da miogenina, que leva à diferenciação terminal dos mioblastos e a via Jak-Stat3, a qual desempenha um papel duplo na proliferação e diferenciação dos mioblastos.

Os dados obtidos *in vitro* sugerem um aumento significativo dos níveis de expressão da proteína Nfix e uma diminuição dos níveis de expressão do gene *Myog*, que codifica para a miogenina, bem como uma desregulação na expressão génica dos genes alvo de ambas as proteínas. Os dados *in vivo* sugerem uma tendência para uma diminuição da expressão do gene *Myog* em amostras de musculo epaxial de ratinhos *dy<sup>W</sup>* e uma tendência para um aumento da expressão do gene *Nfix* no estágio E17.5, assim como uma desregulação na expressão dos seus genes alvo. No estágio E18.5

os dados sugerem uma tendência para uma diminuição da expressão do gene *Nfix* em amostras de músculo epaxial de ratinhos *dy<sup>W</sup>*. O eixo de sinalização RhoA/ROCK-Erk foi descrito como sendo importante na ativação do *Nfix*, e a proteína FAK como sendo importante para a diferenciação dos mioblastos através da ativação do fator regulatório miogénico MyoD e por isso estes fatores foram igualmente alvo de análise *in vitro*. Os níveis de expressão de P-FAK e P-Erk mostram uma tendência para aumento *in vitro* na ausência do gene *Lama2*, assim com *in vivo*, em amostras de músculo epaxial de ratinhos *dy<sup>W</sup>*, no estágio E17.5. Tendo em conta estudos recentes e os resultados obtidos de aumento da expressão de *Nfix* na ausência de *Lama2*, coloca-se a hipótese de que o aumento dos níveis de *Nfix* se deva a uma tentativa de controlo da sobreexpressão da proteína miostatina, a qual inibe a miogénese através da inibição da expressão de *Myf5*, um fator miogénico importante para o processo de diferenciação. Coincidente com a diferenciação comprometida nas linhas celulares C2C12 com o gene *Lama2* silenciado, verificou-se uma retenção significativa de *Myf5* no citoplasma comparando com as células musculares C2C12 selvagens. Contudo é necessário validar no futuro os níveis de expressão génica e proteica da miostatina.

Como mencionado, a via Jak-Stat tem um papel importante na diferenciação dos mioblastos e os resultados obtidos mostram um aumento significativo da expressão da proteína de P-Stat3 *in vitro*, assim como uma tendência para um aumento *in vivo* no estágio E.17.5. Tal está de acordo com estudos anteriores do laboratório que mostraram um aumento de P-Stat3 no músculo fetal de ratinhos *dy<sup>W</sup>*, no estágio E17.5.

Os dados obtidos indicam que a laminina 211 desempenha normalmente um papel na modulação da diferenciação dos mioblastos e a sua ausência leva á desregulação de algumas das vias importantes para a proliferação e diferenciação dos mioblastos. Os resultados sugerem também que a linha celular de mioblastos C2C12 sem o gene *Lama2*, pode ser um bom modelo *in vitro* para LAMA2-CMD, tendo em conta a semelhança com os resultados obtidos *in vivo*, em particular para as amostras de ratinho *dy<sup>W</sup>*, no estágio E17.5.

Um outro objetivo deste projeto foi verificar o impacto da ausência de *LAMA2* em linhas celulares tumorais de melanoma e cancro colorectal, uma vez que ambas foram descritas como tendo alterações na expressão de *LAMA2*. Tendo sido descrito como significativamente expresso em melanoma e cancro colorectal e promover a proliferação e migração, o gene *ENO1* que codifica para a enolase alfa foi analisado e verifica-se uma tendência para diminuição de expressão nas linhas tumorais de melanoma, o que poderá indicar que na ausência de *LAMA2*, há uma diminuição na proliferação e migração. Tendo em conta os resultados obtidos nas células musculares esqueléticas verificou-se também os níveis de expressão da proteína P-Stat3 para a linha tumoral colorectal e verifica-se igualmente uma tendência para um aumento da sua expressão, na ausência de *LAMA2*. Os dados sugerem um ponto chave na ausência de *LAMA2* nas MEC, sendo que independentemente do tipo celular e da doença há um aumento da expressão da proteína P-STAT3 quando há ausência da Laminina 211/221.

Identificar estas vias e mecanismos é essencial para o desenvolvimento de terapias que tenham como alvo direto o início destas doenças.

**Palavras-Chave:** *LAMA2*, LAMA2-CMD, Matriz extracelular, diferenciação, *Nfix*.

## List of Figures and Tables

**Figure 1.1: Extracellular matrix and laminins**

**Figure 1.2: Skeletal muscle development**

**Figure 1.3: Important pathways influencing muscle formation**

**Figure 3.1: Absence of *Lama2* alters *myogenin* pathway *in vitro*, and to a lesser extent *in vivo*.**

**Figure 3.2: Absence of *Lama2* alters Nfix pathway *in vivo* and *in vitro*.**

**Figure 3.3: Impact of *Lama2*-deficiency in Pax7 expression and Myf5 localization in myoblasts.**

**Figure 3.4: *Lama2*-deficiency impacts RhoA and Erk pathways *in vitro*.**

**Figure 3.5: Notch and Myostatin pathways in the absence of *Lama2* absence in C2C12 cells and fetal muscle samples.**

**Figure 3.6: Deletion of *Lama2* delays myoblast differentiation.**

**Figure 3.7: Jak-Stat pathway in the context of *Lama2*-deficiency in C2C12 cells and fetal muscle samples.**

**Figure 3.8: *Lama2*-deficiency impacts FAK pathway *in vitro* and *in vivo*.**

**Figure 3.9: Impact of LAMA2-deficiency in melanoma and colorectal cancer cells.**

**Figure 4.1: Model for MuSC/myoblast differentiation defect in LAMA2-CMD.**

**Table S1 PCR protocol for mouse genotyping.**

**Table S2 List of primers used for genotyping**

**Table S3 List of primers used in Real-Time qPCR analyses**

**Table S4 Real-Time PCR protocol used in CFX96™**

**Table S5 Antibodies and dilutions used for Western Blot and Immunofluorescence**



## List of abbreviations and symbols

°C - Degrees Celsius

**Arbp0** – Acidic ribosomal phosphoprotein  
PO

**Bmp4** - Bone morphogenetic protein 4

**BSA** - Bovine Serum Albumin

**cDNA** - Complementary DNA

**Ckm** - Muscle creatine kinase

**Ct** - Cycle threshold

**DAPI** - 4',6-diamidino-2-phenylindole

**DLL1**- Delta-like ligand 1

**DTT** – Dithiothreitol

**DM** – Differentiation Medium

**DMEM** - Dulbecco's Modified Eagle's  
Medium

**E17.5** - Embryonic stage 17.5

**E18.5** - Embryonic stage 18.5

**ECM** - Extracellular Matrix

**Eno3** - Enolase-β

**FAK** – Focal adhesion kinase

**FBS** - Fetal Bovine Serum

**Fgfs** - Fibroblast growth factors

**GLP4** - Glypican 4

**HRP** - Horse Radish Peroxidase

**HSPCs** - hematopoietic stem and  
progenitor cells

**HSPG** - Heparan sulphate proteoglycan

**kDa** - Kilodalton

**KO** - Knockout

**Jak-Stat** - Janus kinase signal transducer  
and activator of transcription

**LAMA2-CMD** - LAMA2-deficient  
congenital muscular dystrophy

**Lama2 Ko** - *Lama2* knockout C2C12 cells

**LE** - Laminin-type epidermal growth  
factor-like domain

**LG** – Laminin G-like domain

**LN** - Laminin N-terminal domain

**LOX** - Lysyl Oxidase

**M** – Molar

**MDs** – Muscular dystrophies

**mg** - Milligram

**Min** – Minutes

**mL** – Millilitre

**MMPs** - Metalloproteinases

**MRF** - Myogenic regulatory factors

**mRNA** - Messenger RNA

**MuSC** - Muscle stem cell

**MyhC-I** - myosin heavy chain

**nm** – Nanometre

**Nfl** – Nuclear Factor I

**Nfix** – Nuclear factor one X

**PBS** - Phosphate-Buffered Saline

**PCR** - Polymerase chain reaction

**pH3** - Phospho-Histone 3

**PM** – Proliferation medium

**pStat3 Tyr 705** - STAT3 phosphorylated at  
tyrosine 705

**PVDF** - Polyvinylidene Fluoride

**Rpm** - Rotations per minute

**RT-qPCR** - Real time qPCR

**SDS-PAGE** - Sodium Dodecyl Sulphate-  
Polyacrylamide Gel Electrophoresis

**Sec** – Seconds

**Shh** - Sonic Hedgehog

**Sox6** - SRY-Box Transcription Factor 6

**TBST** - Tris Buffered Saline 0,1% Tween

**Tgfβ** - Transforming growth factor β

**WB** - Western Blot

**WT**- Wildtype

**μl**- Microliter

## 1. Introduction

### 1.1 Laminin's role in the extracellular matrix (ECM)

The extracellular matrix (ECM) is an intricate acellular network present in all tissues which provides a physical scaffold for cells.<sup>1-3</sup> Although the ECM is tissue-specific and markedly heterogeneous, it is primarily composed by water, glycoproteins (e.g., collagens, fibronectin, and laminins), elastins, proteoglycans, hyaluronan, and other components collectively termed *matrisome*.<sup>4</sup> There are two major types of ECM, the interstitial matrices and the basement membranes (BMs), a type of matrix that is in close contact with cells (Figure 1.1A).<sup>5</sup>

Interstitial matrices are a gel-like scaffolds characterized by a tissue-specific mixture of a variety of collagen types, fibronectin, elastins, tenascins, proteoglycans and glycosaminoglycans, providing tensile strength, regulation of cell adhesion, mediating migration, and tissue development as well as protection, maintaining extracellular homeostasis and water retention.<sup>5,6</sup>

Basement membrane is a specialized type of ECM that has remarkably diverse functions adapted to individual tissues and organs. Spatially, basement membrane underlies epithelial and endothelial cells, surrounds muscle, fat, and Schwann cells.<sup>7</sup> Composed primarily of laminins, collagen type IV, nidogen and perlecan, a heparan sulphate proteoglycan (HSPG), basement membranes are sheet-like structures which separate these cell types from the surrounding connective tissue.<sup>5</sup> They are important for tissue integrity, stabilizing cells and tissues, linking the ECM to the cytoskeleton.<sup>8</sup> BMs also provide elasticity, biochemical and mechanical signalling, facilitating intra- and intercellular interactions and allow for the linking of structural components to the cell surface.<sup>8</sup>

The communication between ECM molecules and cells is achieved through transmembrane proteins such as integrins, syndecans and dystroglycan.<sup>9</sup> On the extracellular side, these transmembrane proteins bind directly to specific domains of ECM components and, on the intracellular side, they bind to cytoskeletal proteins and different kinases, allowing the transmission of signalling cascades.<sup>4</sup>

The ECM assembly process is dynamic and is particularly evident during embryogenesis where *de novo* accumulation of matrix and subsequent remodelling occurs throughout and accompanies emerging tissues and branched organs.<sup>5</sup> ECM remodelling is a normal process that allows progressive tissue and organ formation and ensures tissue healing and repair. This process occurs through the synthesis and deposition of ECM molecules, the degradation of ECM components, mediated by enzymes such as metalloproteinases (MMPs), and shaping of ECM structure, for example through the action of Lysyl oxidase (LOX) enzymes.<sup>3</sup>

Since ECM provides diverse biological functions, deregulation of important ECM molecules and/or the normal ECM remodelling processes can lead to the loss of normal tissue structure, promoting oxidative stress and the development of different pathological conditions such as fibrosis, diabetes, muscular dystrophies, and cancer.<sup>4</sup>

Laminins are heterotrimeric glycoproteins with approximately 900 kDa composed of a combination of three laminin chains, namely  $\alpha$ ,  $\beta$  and  $\gamma$  chains. There are four different  $\alpha$  chains, and three different  $\beta$  and  $\gamma$  chains and the combination of these chain isoforms leads to the 15 different types of laminins that are known to exist.<sup>10</sup> Depending on the laminin trimer composition, different types of laminin tertiary structures form, the most common being cross-shaped, Y-shaped or rod-shapes. The differences in heteromeric laminin structures are mainly dictated by differences in  $\alpha$ -chains<sup>11</sup> (Figure1.1B).

The cross-shaped laminins, present at the end of the long arm  $\alpha$  chain a C-terminal globular domain with five modules known as laminin G (LG) domains. The homologous short arms are composed of a distal laminin N-terminal (LN) domain followed by tandem repeats of laminin-type epidermal growth factor-like (LE) domains and are essential for laminin polymerization and basement membrane assembly<sup>12</sup> (Figure1.1A). Laminin-211 and 221 are the main isoforms of laminin expressed in healthy adult skeletal muscle.<sup>13</sup> Laminin 211 is composed of an  $\alpha 2$  chain, a  $\beta 1$  chain and a  $\gamma 1$  chain ( $\alpha 2\beta 1\gamma 1$ ) and is present mainly in all myogenic tissues, peripheral nerves

and mesangial matrix of glomerulus and laminin 221 composed of an  $\alpha 2$  chain, a  $\beta 2$  chain and a  $\gamma 1$  chain ( $\alpha 2\beta 2\gamma 1$ ) and is found in neuromuscular junctions, mesangial matrix of the glomerulus and in adult cardiac muscle<sup>11</sup>. The *LAMA2* gene codifies the laminin- $\alpha 2$  chain, which is essential for the production and secretion of laminins 211 and 221 in skeletal muscle.<sup>14</sup> The C-terminal domain of laminin- $\alpha 2$  chain communicates via its five LG domains with the muscle cell cytoskeleton by binding to integrin  $\alpha 7\beta 1$  and the dystroglycan protein complex, stabilizing the basement membrane and enabling laminin polymerization.<sup>11,14</sup> (Figure 1.1C). The N-terminal domain of the laminin- $\alpha 2$  ensures the association of laminins to each other and to additional components of the BM, such as nidogen, collagen IV and perlecan (Figure 1.1C).<sup>14</sup>

Laminins have an important role in the structural support, maintenance, and differentiation of animal tissues, more specifically in creating a primary scaffold that (1) attaches the ECM to the cell surface and (2) serves as a platform to which other ECM components become stably attached. Therefore, binding of laminins to their receptors impacts on the assembly of the basement membrane, mechanical linkage of the cell to the basement membrane and signalling.<sup>15</sup> Modification of the structure of these proteins will lead to basement membrane destabilization, which consequently, will affect these important processes. For example, mutations in the *LAMA2* gene result in various truncations of the laminin- $\alpha 2$  protein which lead to a range of disease phenotypes<sup>15</sup> (*see section 1.4*).

In addition to the structural and mechanical support, ECM and cell-ECM engagement through cell surface receptors, namely laminin-integrin binding, provides signals to the interior of the cells affecting their gene expression as well as diverse cellular responses such as proliferation, polarisation, and differentiation, as exemplified by skeletal muscle development.<sup>5</sup>

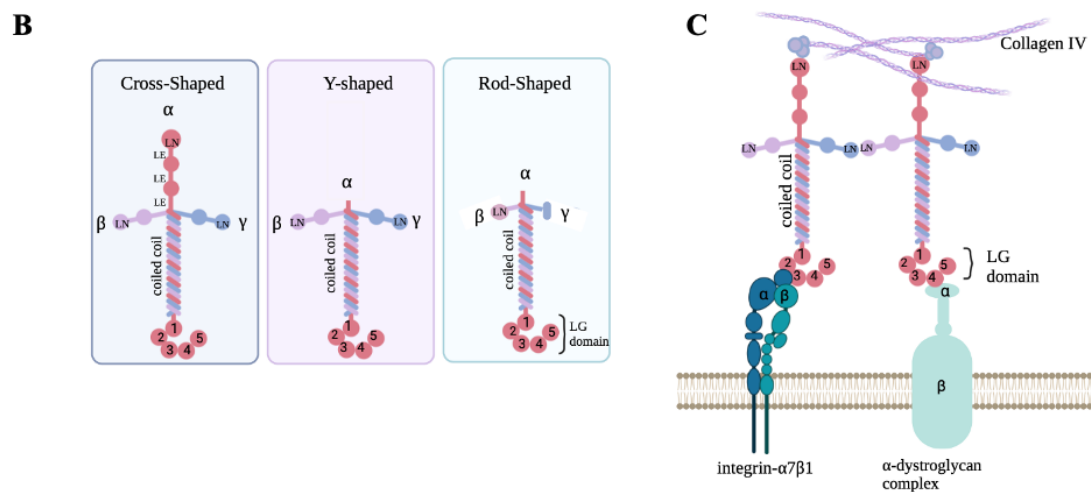
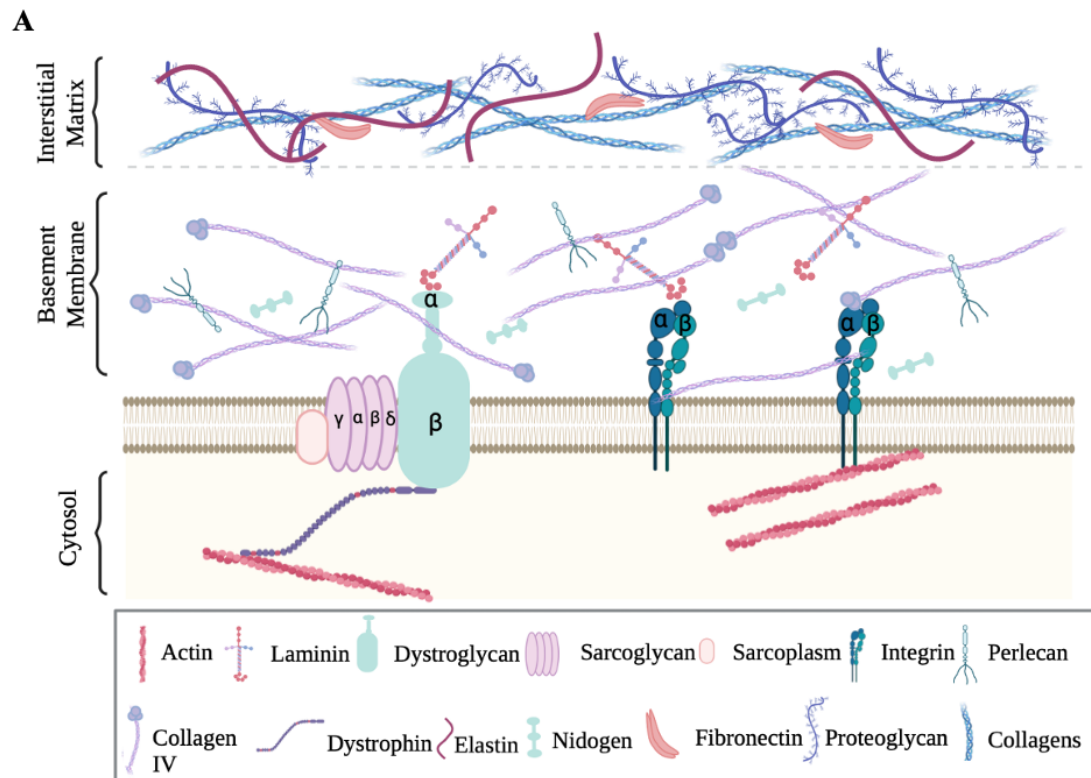


**Figure 2.1: Extracellular matrix and laminins.** (A) ECMs are composed of two different types of matrices: 1) the interstitial matrix, containing collagens, elastin, fibronectin, and proteoglycans; and 2) the basement membrane, which includes perlecan, nidogen, collagen IV and laminins. Communication between ECM and cells is assured by transmembrane receptors: in skeletal muscle, integrins connect to laminins and collagen IV, which connect to the actin cytoskeleton and the dystroglycan-sarcoglycan-sarcoplasm complex links laminins to actin filaments through dystrophins. (B) Schematic representation of the three main types of laminin tertiary structures, determined by the combination of laminin  $\alpha$ ,  $\beta$ , and  $\gamma$  chains: Cross-shaped, Y-shaped, or Rod-shaped. Laminin  $\alpha$ ,  $\beta$ , and  $\gamma$  chains are organized in a coiled coil, the  $\alpha$  chain long arm ends in a combination of five laminin G-like (LG) domains. The  $\alpha$ ,  $\beta$ , and  $\gamma$  short arms have a N terminal domain (LN), followed by tandem repeats of laminin-type epidermal growth factor-like (LE) domains. (C) In skeletal muscle cells, laminin 211 heteromeric proteins bind through their C-terminal domain to muscle cell integrin receptors and the  $\alpha$ -dystroglycan protein complex: LG1-3 domains bind to integrins- $\alpha7\beta1$  and LG 4-5 domains bind to the  $\alpha$ -dystroglycan complex. The laminin- $\alpha2$  N-terminal domain bind to collagen IV while the three short arms of the laminin trimer associate to the short arms of other laminin molecules, forming an assembled laminin sheet.

## 1.2 Myogenesis

ECM molecules play important roles in cell survival and maintenance, and cell-ECM interactions have significant roles during all stages of skeletal muscle development; hence it has been suggested that this “extracellular matrix dimension” should be added to the conceptual network of factors contributing to skeletal myogenesis.<sup>5</sup>

Skeletal muscle is a highly complex and heterogeneous tissue that serves a multitude of functions in the organism. Being the most abundant tissue in vertebrates and distinct from the other types of muscles (smooth and cardiac) because it can be voluntarily controlled by the organism, skeletal muscle is necessary for locomotion, breathing, and energy metabolism.<sup>16</sup> Skeletal muscles are bundles of striated myofibers which are elongated multinucleated syncytia, surrounded by a basement membrane and filled with highly organized cytoskeletal components in the form of myofibrils.<sup>16</sup> The cells which form the skeletal muscles of the trunk and limbs, arise from somites, transient embryonic structures that originate from paraxial mesoderm, whereas muscles of head and neck derive from the anterior paraxial mesoderm.<sup>17</sup>

Myogenesis, the process of generating muscle, encompasses distinct phases and is controlled by cell autonomous and cell–cell communication pathways within the developing skeletal muscle tissue, as well as by signals secreted by surrounding tissues.<sup>18</sup>

Paraxial mesoderm, composed of two bilateral strips of tissue flanking the neural tube and notochord, undergoes segmentation in a rostral to caudal fashion where each segment epithelializes to form balls of cells called somites. Somites then develop into four distinct compartments.<sup>16,18</sup> The dorsal-most compartment, the dermomyotome, contains proliferating progenitors of all skeletal muscles of the body and limbs – the Muscle Stem Cells (MuSCs) – as well as precursors of brown fat, endothelial cells and of dorsal dermis.

The myotomes are formed by delamination of dermomyotomal cells from its edges and are the first differentiated muscle cells to form.<sup>19</sup> MuSCs expressing Pax3 and/or Pax7 at the edges of the dermomyotome are induced to initiate the myogenic program and differentiate into myotomal myocytes.<sup>20</sup> Subsequently, Pax3- and/or Pax7-expressing MuSCs activate the expression of MRFs: *Myf5*, *Mrf4* and/or *MyoD1* and will be committed into myoblasts. These myoblasts proliferate a few times and lead to the expression of the fourth MRF, myogenin (*Myog*), that will promote the differentiation of the myoblasts in myocytes (Figure 1.2).<sup>17</sup> Later, Pax3- and/or Pax7-positive embryonic MuSCs arrive to the myotomes through the de-epithelialization of the central dermomyotome, induced by fibroblast growth factors (Fgfs) secreted from the myotome. Some of these cells stay Pax3- and/or Pax7-positive and continue proliferating, while others activate the myogenic program and differentiated into primary myoblasts which fuse with each other or the myotomal myocytes to form primary or embryonic myotubes. This process is termed primary (or embryonic) myogenesis and occurs between E11.0 and E14.5 in mouse development. Primary myogenesis is essential to organize the basic muscle pattern; muscle fibers are innervated by motor axons and establish the connections to their tendons. Interestingly, myotubes do not present basement membrane nor express laminin receptors during primary myogenesis.<sup>21</sup> Secondary or fetal myogenesis starts at E14.5 in the mouse and proceeds until birth. During this stage *Pax7* positive MuSCs are no longer *Pax3*, and the ones which did not differentiate during primary myogenesis proliferate immensely, and some of them become committed to myoblasts<sup>21</sup>. Then, myoblasts undergo a second wave of differentiation become myocytes and fuse with each other or with the primary myotubes, giving rise to the secondary or fetal myotubes (Figure 1.2).<sup>17</sup> During secondary myogenesis basement membrane is progressively assembled, and an adhesion complex is formed allowing the interaction between the actin cytoskeleton of muscle fibers and laminins, the major constituents of basement membrane, leading to a thin sheet wrapped around the fiber in the end of fetal development.<sup>21</sup> MuSCs differentiation profile alters through the different developmental stages, due to the expression of different specific genes, like nuclear factor one X (*Nfix*), which is activated by Pax7, and promotes the switch between embryonic and fetal myogenesis. *Nfix* has been described as the responsible for the inhibition of specific embryonic expression genes, as *Myh1* (coding for the myosin heavy chain), and the activation of fetal genes as *Eno3* (Enolase- $\beta$ ) and *Ckm* (muscle creatine kinase), downstream targets of *Nfix* pathway.<sup>22</sup>

At the end of the secondary myogenesis secondary myotubes are formed and a pool of MuSCs is kept ensuring myofiber growth.

Postnatally, MuSCs proliferate and some of them differentiate into myocytes which fuse with the preexisting myofibers increasing their size. Perinatal MuSCs are located under the myofiber basement membrane and tend to divide asymmetrically<sup>21</sup>. This allows the production of MuSCs that commit into myoblasts and differentiate in myocytes, that fuse with the preexisting myofibers, contributing to their growth. Also, to MuSCs expressing Pax7 that become satellite cells, a pool of quiescent cells, they appear as mononucleated cells underneath the basement membrane of each individual fiber, these cells are responsible for the postnatal muscle fibers growth and regeneration (Figure 1.2).<sup>22</sup>

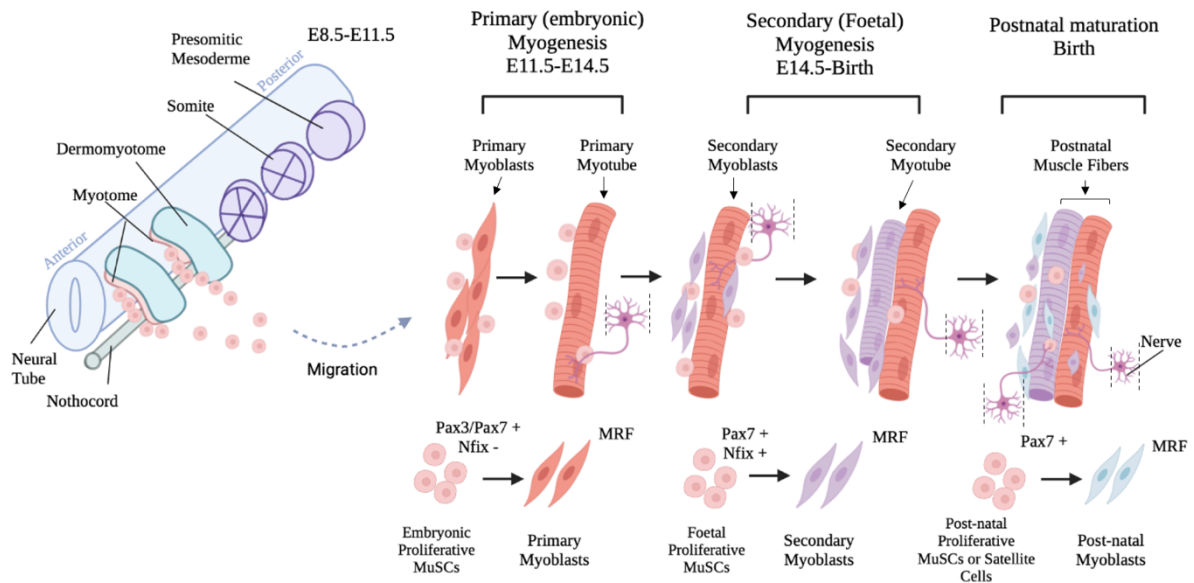


**Figure 1.2: Skeletal muscle development.** Schematic view of amniote muscle formation in trunk and limbs. MuSCs originating from the dermomyotome of the somites translocate underneath the dermomyotome, differentiating and giving rise to segmented myotomes, that later will transform into axial muscles or migrate and differentiate when they reach their target site. Myogenesis has different phases: Myotome formation occurs from E8.5 to E10.5. Primary or embryonic myogenesis starts at E11.5, where Pax3- and/or Pax7-expressing MuSCs activate the designated myogenic regulatory factors (MRFs): Myf5, Mrf4 and/or MyoD and will be committed into primary myoblasts. The primary myoblasts fuse with each other to form primary myotubes. Between E14.5 and birth Pax7-positive MuSCs, undergo a second wave of differentiation. Pax7 activates *Nfix* expression in MuSCs, some of them activate MRFs and differentiate and secondary myocytes fuse with each other giving rise to the secondary or fetal myotubes or with the primary myotubes, increasing their size. From E17.5, secondary myoblasts fuse mostly with existing myotubes to increase their size. During postnatal stages, myotubes continue to grow through fusion of myoblasts and then mature into myofibers. MuSCs expressing Pax7, come to enter quiescence and occupy a position as satellite cells along the myofibers. Innervation of myotubes is schematically represented (Nerve); the cell body of the neuron is located on the spinal cord.

### 1.3 Essential players in skeletal muscle formation

#### 1.3.1 *Nfix*

*Nfix* is a member of the NFI (nuclear factor I) transcription factors family, which in vertebrates consists of four closely related genes – *Nfia*, *Nfib*, *Nfic* and *Nfix* – that are involved in the control of gene expression in a variety of cell types and tissues. Binding sites for NFI proteins are present in genes expressed in the brain, muscle, liver and mammary gland.<sup>23,24</sup> NFI proteins bind to DNA recognizing the consensus site TTGGC(N5)GCCAA with the same apparent affinity, being implicated in gene activation and repression, although the mechanisms by which they act as activators or repressors remain unknown. A highly conserved N-terminal DNA-binding and

dimerization domain is encoded by all four genes while the C-terminal transactivation domains of each NFI family member is much less conserved.<sup>25</sup> NFI proteins bind to DNA either as homodimers or heterodimers with other family members through a N-terminal region.<sup>25</sup>

Nfix is a key factor with a dual role in skeletal muscle development, most exactly on the transition from embryonic to fetal environment, inhibiting the expression of embryonic specific genes on myoblasts and promoting the expression of the fetal ones (Figure 1.3A). A recent study reports that RhoA through the activation of its major effector, ROCK, represses Erk kinase activity leading to JunB (a member of AP-1 family) activation, and this last factor regulates Nfix expression during fetal development.<sup>26</sup> In turn, Nfix mediates the activation of the fetal muscle specific genes *Ckm* and *Eno3*, in mice (Figure 1.3A). Nfix physically interacts with protein kinase C $\theta$  (Pkc $\theta$ ) and myocyte enhancer factor-2A (Mef2A), enabling the latter to bind to the *Ckm* promoter and activate its transcription.<sup>27</sup> On the other hand, by interacting with SRY-Box Transcription Factor 6 (Sox6) that functions as a co-repressor, Nfix represses the expression of embryonic specific genes such as *MyHC-I*, which is expressed in embryonic myotubes and defines the slow muscle fibers during development, so that this myosin isoform is not expressed in fetal myotubes (Figure 1.3A).<sup>27</sup>

In addition to being involved in skeletal muscle development, Nfix has also been reported to play a role in some diseases associated with muscle wasting and damage, such as muscular dystrophies.<sup>28</sup> It has been reported that after cycles of degeneration, Nfix overexpression in dystrophic mice muscles increases regeneration, and as a consequence of the attempt to repair damage, satellite stem cells that, unfortunately, share the same mutation of the myofibers, are not able to successfully repair the damage leading to the loss of muscle tissue and establishment of fibrosis, exacerbating markedly the pathology.<sup>28</sup>

Apart from skeletal muscle, Nfix is also highly expressed in the embryonic mouse telencephalon, throughout embryogenesis, in cells within the cerebellum and spinal cord, as well in mature neuronal populations in postnatal and adult cerebellum.<sup>24</sup>

Nfix was also identified as an important factor in hematopoietic stem and progenitor cells (HSPCs).<sup>25</sup> Depletion of *Nfix* significantly reduces the colony-forming potential and repopulation activity of HSPCs, suggesting that Nfix may be a regulator of HSPCs survival.<sup>25</sup> Recent studies also suggest that Nfix contributes to prostatic hyperplasia, through its interacting with FoxA1, regulating prostate specific gene expression.<sup>29</sup> In addition, Nfix was implicated as a tumor-suppressor gene in colorectal cancer and squamous cell carcinoma,<sup>25</sup> and in lung cancer, Nfix was identified as the master regulator, strongly associated with 17 genes involved in the migration and invasion pathways including IL6ST, TIMP1 and ITGB1.<sup>30</sup>

### 1.3.2 Myostatin

Another critical regulator of the prenatal and postnatal myogenesis is Myostatin, a secreted factor of the transforming growth factor  $\beta$  (Tgfb $\beta$ ) superfamily, that has recently been described to be regulated by Nfix at the transcriptional level, and which controls the temporal progression of muscle regeneration in injured mice.<sup>22</sup> Myostatin negatively regulates muscle growth and loss-of-function mutations in the gene encoding Myostatin (*Mstn*) result in a dramatic increase of muscle mass in different species, including humans.<sup>31</sup> Studies using myogenic cell lines show that Myostatin inhibits myoblasts proliferation, by activating the cyclin-dependent kinase inhibitor p21, which forces cell cycle exit (Figure 1.3B).<sup>32</sup> Simultaneously, Myostatin activation is associated with a strong inhibition of myogenic differentiation, and consequently controls skeletal muscle tissue growth.<sup>32</sup> In mice, the inactivation of the Myostatin gene doubles skeletal muscle mass and conversely, systemic overexpression leads to a muscle wasting syndrome, characterized by extensive muscle loss.<sup>31</sup>

Myostatin plays a key role in skeletal muscle homeostasis and can act through three distinct intracellular signaling pathways: 1) it can modulate MyoD/myogenin expression through phosphorylation of signal transducer and activator of transcription 2/3 (SMAD2/3) that will block MyoD production reducing myoblast proliferation, differentiation, and fusion (Figure 1.3B)<sup>33</sup>; 2)

it can inhibit AKT, which leads to FoxO1 downregulation and consequently an increase of atrogenin, a muscle specific ubiquitin ligase, increasing myoblast degradation,<sup>33</sup> and 3) Myostatin inhibition of AKT can also lead to muscle hypertrophy by increasing mTOR or inhibiting GSK-3 $\beta$  expression, which will lead to an increase in satellite cells synthesis.<sup>33</sup>

### 1.3.3 Jak-Stat

Similar to the factors already described as essential in skeletal muscle formation, by critically controlling the onset of myogenic differentiation<sup>33</sup> Janus kinase (Jak)/signal transducer and activator of transcription (Stat) pathways have been shown to be involved in mammalian myogenic differentiation in two opposite manners. One pathway, consisting of Jak1/Stat1/Stat3 activation, promotes myoblasts proliferation and inhibits their differentiation, through nuclear entry of phosphorylated Stat3 which inhibits the expression of specific genes controlling myoblasts differentiation. The other pathway consisting of Jak2/Stat2/Stat3 activation, involves the presence of Socs1 and 2 and Pias1 which prevent Stat3 phosphorylation and consequently promote myogenic differentiation (Figure 1.3C).<sup>34</sup>

Recent studies have reported that deletion of the *Stat3* gene leads to reduced levels of the MRF MyoD and myogenin *in vitro*, and *Stat3* deletion *in vivo* caused impairment of post-traumatic muscle regeneration.<sup>35</sup> *In vivo* studies also report that Stat3 activated by interleukin-6 (IL6), regulates satellite cell behavior, promoting myogenic progression through myogenic differentiation 1 (MyoD1) regulation, indicating Stat3 as a key factor for the renewal of satellite cells in injured muscles.<sup>36</sup>

### 1.3.4 FAK

Focal adhesion kinase (FAK) is a well-studied protein that responds to changes in cell-ECM engagement and cellular tension. Through multifaceted and diverse molecular connections, FAK can influence the cytoskeleton, the structural properties of cell adhesion sites and membrane protrusions to regulate cell movement.<sup>37</sup> In skeletal muscles, FAK is enriched at the costameres and the myotendinous junction, which are the main force transducers of skeletal muscle.<sup>38</sup> Multiple roles have been attributed to this protein in skeletal muscles, such as being activated by receptor tyrosine kinases for growth factors and to regulate myoblast differentiation and muscle fiber formation. FAK signaling enhances de promyogenic factor Cdo expression positively regulating N-Cadherin/Cdo-mediated cell adhesion signaling during myoblasts differentiation.<sup>39</sup> Also, FAK signaling induces Cdc42 that promotes filopodia formation which are formed dynamically during myoblast differentiation and play important role in myoblasts fusion (Figure 1.3D).<sup>39</sup> FAK activity was shown to alter cell cycle progression and differentiation commitment of MuSCs<sup>38</sup>.



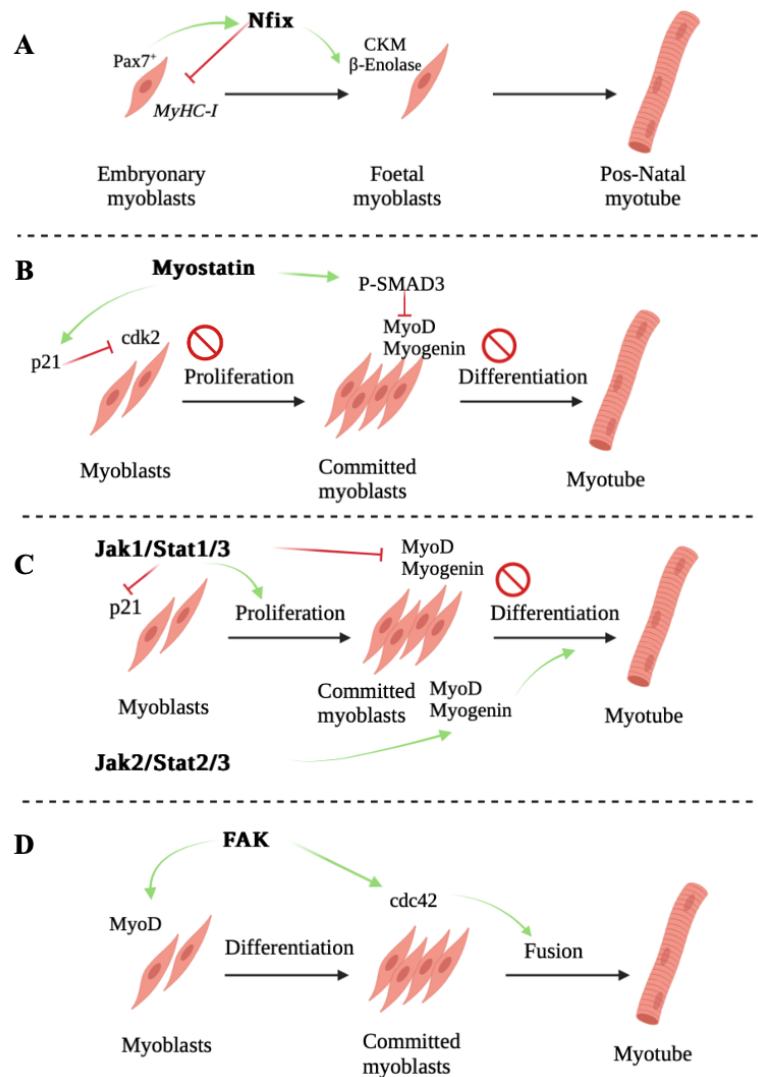


**Figure 1.3: Important pathways influencing muscle formation.** **A:** Nfix activated by Pax7 allows the switch between embryonic and fetal myogenesis. **B:** Myostatin, a negative regulator of muscle mass, inhibits myoblasts proliferation through the activation of p21 and impacts myoblasts differentiation inhibiting the expression of MRFs MyoD and Myogenin. **C:** Jak/Stat pathway impacts differentiation in two opposite ways, the Jak1/Stat1/Stat3 pathway inhibits differentiation and promotes myoblasts proliferation, the Jak2/Stat2/Stat3 pathway is required for myogenic differentiation. **D:** FAK is an important factor for myoblasts differentiation through MyoD activation and is necessary for myotube formation by activating Cdc42 that allows myoblasts fusion.

#### 1.4 ECM mutations and muscular dystrophy

As mentioned before, in skeletal muscle, the link between the ECM and the cytoskeleton occurs through transmembrane proteins, including integrins, syndecans and dystroglycan, which interact with cytoplasmic components, as represented by dystroglycan which forms a glycoprotein complex with the cytoplasmic protein dystrophin.<sup>5</sup> This structure is critical to stabilize cells and tissues, providing a solid-phase cell adhesion to the ECM. Therefore, is not surprising that mutations in components of the dystrophin-glycoprotein complex, skeletal muscle basement membrane or the transmembrane receptor proteins can cause several forms of muscular dystrophies.<sup>40</sup>

The muscular dystrophies represent a group of autosomal recessive disorders, causing muscle weakness (hypotonia) and atrophy and are often inherited. *LAMA2* congenital muscular dystrophy (LAMA2-CMD), is the most common congenital muscular dystrophy and is triggered by mutations in the *LAMA2* gene, codifying the  $\alpha 2$  chain of laminin 211.<sup>41</sup> The main laminin

receptors expressed on cell surfaces are dystroglycan, integrin complex and sulfated glycolipids.<sup>15</sup> In a context of laminin-deficient muscular dystrophy this binding of laminins to their receptors is compromised, affecting basement membrane assembly, mechanical linkage of the cell to basement membrane and signaling.<sup>15</sup> Because of laminin- $\alpha$ 2 deficiency, myofibers become damaged and to compensate for the muscle injury, satellite cells are activated, leading to myofiber regeneration, but muscle fibers undergo apoptotic degeneration followed by regeneration and chronic inflammation.<sup>15</sup> Therefore, muscle tissue is replaced by connective tissue, fibrotic tissue, and adipocytes.<sup>41</sup>

Using a mouse model for human LAMA2-CMD, the *dy*<sup>W</sup> mouse, the host laboratory and collaborators have shown that the disease onset occurs between mouse developmental stages E17.5 and E18.5, with a dramatic drop in the number of Pax7- and myogenin-positive cells within *dy*<sup>W</sup> muscles.<sup>20</sup> It was also observed that E18.5 *dy*<sup>W</sup> muscles are smaller and do not recover in size postnatally.<sup>20</sup> This may be explained via an overactivation of Jak-Stat signaling, which was hypothesized to promote disease onset and progression.<sup>20</sup>

Apart from Jak-Stat signaling deregulation, alterations in other essential pathways involved in myogenesis is also shown to be linked to muscular dystrophies. Recent studies have shown that silencing *Nfix* postnatally in both dystrophic  $\alpha$ -sarcoglycan (*Sgca*-null, a model for limb-girdle muscular dystrophy type 2D) – and dystrophin (*mdx*, a model for Duchenne muscular dystrophy)-deficient mice protects their muscle fibers from degeneration.<sup>28</sup> Using the *mdx* dystrophic mouse, it has also been reported that during regeneration in the *mdx* dystrophic mouse model, *Nfix* regulates *Mstn* (Myostatin gene), a negative regulator of skeletal muscle mass, directly inhibiting and hence controlling the temporal progression of the regeneration process.<sup>22</sup> In *Sgca*-null and *mdx* mice, *Nfix* is expressed after ROCK-dependent phagocytosis in macrophages, inducing a decrease of pro-inflammatory markers and an increase of anti-inflammatory ones in these cells, being responsible for their phenotypic switch.<sup>42</sup> Accordingly, *Nfix* deletion in macrophages protects muscle fibers and inhibits fibrosis, by reducing the anti-inflammatory macrophages and consequently preventing the Tgf $\beta$ - mediated ECM deposition.<sup>42</sup> *Nfix* is therefore a promising factor to target in dystrophic diseases, since it reduces severity of symptoms.<sup>41</sup>

### 1.5 ECM mutations and Cancer

Due to the critical importance of the ECM for tissue structure and stability, dysregulation of ECM dynamics leads not only to muscular dystrophies, but can also cause several other diseases, including cancer.<sup>3</sup> In cancer cells, small changes in the homeostasis of their microenvironment can have significant effects. For example, collagens, important ECM components that dictate primary functional properties of the matrix, are crucial for cancer proliferation, and changes in their deposition or degradation lead to loss of ECM homeostasis.<sup>43</sup> Laminins are also heavily involved in tumor angiogenesis, cell invasion, metastasis development and drug resistance.<sup>44</sup> Recent studies demonstrated that certain *LAMA2* gene mutations correlate with melanoma metastasis<sup>45</sup> and to lung adenocarcinoma metastasis via PI3K/AKT pathway.<sup>46</sup>

Due to the importance of the ECM in the control of cell behavior and differentiation<sup>3</sup>, it is not surprising that pathways involved for example in muscle development are also altered in cancer. Recent studies show that *Nfix* upregulation might be associated with chemoresistance in colorectal cancer cells and in triple negative breast cancer, *Nfix* can interact and cooperate with MECP2 to suppress the expression of desintegrins, which are modulators of integrin-ECM engagement.<sup>47</sup> In the same way, Jak-Stat activation has been shown to contribute to acquisition of properties required for tumor invasion and metastasis, in part mediated by the activation of the epithelial to mesenchymal transition (EMT) which is also involved in embryonic development.<sup>48</sup> Moreover, recent studies demonstrate that FAK controls fundamental cellular processes like cell adhesion, migration, proliferation, and survival, and promotes important malignant features in cancer progression like EMT, tumor angiogenesis, chemotherapeutic resistance, and stromal fibrosis.<sup>49</sup>

## 1.6 Aims of the project

Previous studies in the host laboratory defined the time for the onset of LAMA2-CMD in the *dy<sup>w</sup>* mouse model, which coincides with a dramatic drop in Pax7- and myogenin-positive cells and an overactivation of Jak-Stat signaling in fetal skeletal muscles.<sup>20</sup> The next step is to understand exactly which signaling pathways are affecting MuSCs/myoblasts and their correct development, and how these events trigger the onset of the disease. In particular, this Master thesis project aims to investigate how *Lama2*-deficiency affects MuSC/myoblast differentiation. To accomplish this goal, the following tasks were defined:

- Dissect out which pathways, normally involved in myoblast differentiation (Nfix, Myogenin, Jak-Stat, Myostatin and FAK), are altered in the absence of *Lama2 in vivo*.
- Explore the C2C12 myogenic cell line as an *in vitro* model for LAMA2-CMD and validate the targets found to be differentially expressed *in vivo*.
- Analyze if the pathways altered in LAMA2-CMD myoblasts are also altered in *LAMA2*-deficient cancer cell lines.

With this work we expect to move closer to understanding the molecular or cellular mechanism(s) underlying the first steps of the disease in *Lama2*-null muscles. These could be essential for the development of therapies that target the primary mechanisms of the disease.

## 2. Material and Methods

### 2.1 Mice and fetus collection

The genetically modified ( $dy^W$ ) mice used in the project (license number 0421/000/000/2022, DGAV) are the most studied and frequently used mouse model for LAMA2-CMD pathogenesis<sup>50</sup> ([www.curecmd.org/resources-for-scientists](http://www.curecmd.org/resources-for-scientists)). Colony breeding (Ethics Protocol A005-2019) was performed at Instituto Gulbenkian Ciência in a specific pathogen free animal facility and heterozygous crossings were done at FCUL (Ofício n° 99 0420/000/0009/11/2009). Heterozygous  $dy^{W+/-}$  C57BL/6 mice were crossed to obtain homozygous  $dy^{W-/-}$  mutants and wildtype fetuses, which were sacrificed at E17.5 or E18.5 after which epaxial muscles were isolated for subsequent analysis. Pregnancy was confirmed by the presence of a copulation plug on E0.5 and by weighing the females before they were sacrificed. This was performed by licensed team members (DGAV, DL113/2013). Pregnant females were anesthetized via inhalation of isoflurane and sacrificed by cervical dislocation. Uterine horns were removed and placed in ice-chilled PBS, fetuses were dissected out and decapitated and tails were cut for genotyping. Deep back muscles were isolated from the fetuses and used in different experimental setups or kept at  $-80^{\circ}\text{C}$  for long-term preservation. These samples are designated as epaxial muscle and are samples of whole muscle that will be described on this project as *in vivo* samples in E17.5 or E18.5.

Our research was conducted in agreement with the European Directive 2010/63/EU and Portuguese legislation (Decreto-Lei 113/2013, Decreto-Lei 1/2019).

#### 2.1.1 Genotyping

Mice from the breeding colony were marked by an ear punch used to identify the animals and tissue from tails was also used for genotyping and placed into Eppendorf tubes. Next, 25 mM NaOH / 0,2 mM EDTA was added to the samples and placed in thermocycler at  $95^{\circ}\text{C}$  for 30 min, followed by cooling tubes to  $4^{\circ}\text{C}$ . Then, 40 mM Tris HCl pH 5,5 was added to the mixture in a 1:1 ratio and centrifuged at 4000 rpm for 3 min. For PCR, 1 $\mu\text{l}$  of undiluted mixture was used per reaction. All PCR reactions (protocol in Table S1, Annex) were performed using Xpert Fast Hotstart DNA Polymerase (GRISP) according to the manufacturer's instructions. A single mix was prepared with the primers listed in Table S2 (Annex).

### 2.2. In Vitro approach

#### 2.2.1. C2C12 cell line

C2C12 cells are a well-established cell line derived from mouse skeletal muscle satellite cells and is often used to study myogenic processes.<sup>51</sup> In this project, C2C12 *Lama2*-deficient cell lines were used as an *in vitro* model for LAMA2-CMD. The deletion of *Lama2* gene from C2C12 cell lines, was previously generated in the host laboratory with CRISPR-Cas9 vectors targeting *Lama2* and single cell clones were established (*Lama2* KO C2C12 cells).<sup>52</sup>

#### 2.2.2 Cancer cell lines

In this project two cancer cell lines were used: A375: (1) a human melanoma cell line initiated through explant culture of a solid tumor from a 54-year-old female, kindly provided by UIMP-IPO (Unidade de Investigação em Patobiologia Molecular, Instituto Português de Oncologia de Lisboa), and (2) HCT116 (a kind gift from Luís Ferreira Moita), a human colorectal carcinoma cell line initiated from an adult male. Both cell lines are adherent with an epithelial morphology. The host laboratory previously generated knockout cell lines for *LAMA2* from A375 and HCT116 cell lines using CRISPR-Cas9 vectors targeting *LAMA2*, and single cell clones were established (Inês Fonseca, Master thesis, ongoing). Briefly, cells were co-transfected with CRISPR-Cas9 vectors and a vector containing a selection marker (Puromycin or GFP) and selected 48h after transfection. Positively transfected cells obtained after selection are referred to in this thesis as pool. From these transfected cells, single cell clones were also established in order to obtain defined *LAMA2* knockout cell lines (referred to in this thesis as KO).

### 2.2.3 Cell Culture

Cells were grown in Dulbecco's Modified Eagle's Medium (DMEM), supplemented with 10% fetal bovine serum (FBS) and 1% of an antibiotic mixture: Penicillin (10000U/ml) and Streptomycin (10mg/ml) (complete or proliferation medium). The cell lines were maintained in culture at 37°C, 5% CO<sub>2</sub>, constant humidity and when 70% of confluency was reached, trypsin-EDTA was used to split the cells.

### 2.2.4 Differentiation assay

On day 0, wildtype (WT) and Lama2-deficient (KO clones) C2C12 cells were plated in proliferation medium, DMEM (Dulbecco's Modified Eagle's Medium) supplemented with 10% FBS (fetal bovine serum) and 1% of an antibiotic mixture: Penicillin (10000U/ml) and Streptomycin (10mg/ml) (complete medium), at a density of 50.000 cells per well in a 24-well plate with coverslips. On day 1 the medium was changed to differentiation medium (DMEM supplemented with 2% of horse serum and 1% of an antibiotic mixture: Penicillin (10000U/ml) and Streptomycin (10mg/ml) (complete medium) and left until day 5. The cells were imaged on days 0, 1, 2 and 5 using an Olympus CK2 microscope and a MilkroOkular Full HD camera. On day 5, cells were fixed for immunofluorescence (see section 2.5. *Immunofluorescence*).

## 2.3 Real Time-qPCR

### 2.3.1 RNA extraction

Epaxial muscles, previously isolated from fetuses and stored at -80°C, were homogenized in 500 µl of TRIzol™ Reagent (Invitrogen™) using a tissue homogenizer (Retsch MM400 Tissue Lyser). C2C12 cells were directly lysed in 500 µl of TRIzol™ reagent. Upon dissociation of the nucleoprotein complexes, 100 µl of chloroform was added to separate the lower red phenol-chloroform, the interphase, and the colorless upper aqueous phase. For that, samples were incubated for 2-3 min and centrifuged for 15 min at 12,000g at 4°C. The aqueous phase containing the RNA was transferred into a new tube. For epaxial muscle samples, the interphase and the organic phase was saved to proceed with a protein extraction protocol (see section 2.3.1 *Protein extraction a) tissue samples* below). To precipitate RNA, 250 µl of isopropanol were added to the aqueous phase, and samples were incubated for 10 min. Then samples were centrifuged for 10 min at 12,000 g at 4°C. The supernatant was discarded, the pellet was washed twice with 500 µl of 75% ethanol and centrifuged for 5 min at 7500 g at 4°C. The ethanol was subsequently removed, the pellet was air dried, resuspended in 20–50 µl of RNase-free water and placed on ice. Samples were then incubated at 55°C for 10 min and returned to ice. RNA concentrations and quality were determined with Nanodrop1000.

### 2.3.2 cDNA and RT-qPCR

The Xpert cDNA Synthesis Kit (GRiSP) was used to synthesize complementary DNA (cDNA) from a single-stranded RNA template (obtained in the previous section 2.2.1 *RNA extraction*). The initial reaction mixture contained the following components: 1µl dNTP mix, 1µl random hexaprimers, RNase free water and 1µg RNA obtained after RNA extraction. Subsequently, 4 µl 5X reaction Buffer, 0,5 µl of RNA inhibitor (40U/ µl) and 1,0 µl Xpert RTase (200U/ µl) were added to the mixture, mixed thoroughly, briefly centrifuged and placed in a thermocycler at 25°C for 10 min, 50°C for 50 min and 85°C for 5 min. The cDNA obtained was stored at -20°C until further analysis by Real-Time qPCR (RT-qPCR).

RT-qPCR reaction was performed using SsoAdvanced Universal SYBR® Green Supermix or iTaq™ Universal SYBR® Green Supermix (Bio-Rad). Reaction mixture of qPCR was prepared with the following components (total of 10 µl per reaction): 5 µl of Universal SYBR Green Supermix (2x), 0,4 µl of forward and 0,4 µl of reverse primers and 3,2 µl of nuclease-free H<sub>2</sub>O. All reaction components were thawed beforehand, thoroughly mixed and stored on ice, protected from light. Primer sequences used are listed in Table S3 (Annex). The mixture was then distributed into wells of a 96-well plate and 1 µl of cDNA was added to each well. The plate was sealed with an optically transparent film and centrifuged to remove air bubbles and to ensure that the volume of mixture stayed at the bottom of the well. Each sample was run in duplicate. Finally,

a CFX96™ Real-Time PCR Detection System (Bio-Rad) was used to perform the RT-qPCR reaction using the protocol in Table S4 (Annex). Data analysis of the PCR run was performed by analyzing the threshold cycle (Ct) values and comparing the Ct value of the gene of interest (GOI) and the housekeeping gene, according to the following equations:

$$\Delta Ct = Ct_{\text{housekeeping}} - Ct_{\text{GOI}} \quad (2.1)$$

$$\text{Fold difference to housekeeping} = 2^{\Delta Ct} \quad (2.2)$$

The quality of all PCR reaction was assessed by melting curve analysis.

## 2.4 Western Blot

### 2.4.1 Protein extraction

#### a) *Tissue Samples*

As mentioned before (2.2.1 RNA extraction) the interphase and organic phase obtained during the RNA extraction procedure were kept in the microcentrifuge tubes to proceed with protein extraction. This is in compliance with the 3R policy of animal welfare, where the same fetal muscle sample was used for both RNA and protein extraction. First, the remaining aqueous phase (containing RNA) left in the tube was removed. To precipitate the DNA, 150 µl of 100% ethanol was added and the tube was mixed by inversion. The mixture was centrifuged for 5 min at 2000 g at 4°C and the phenol-ethanol supernatant containing the proteins was transferred into a new tube, to proceed with protein isolation. To precipitate the proteins, 750 µl of isopropanol was added, the sample was incubated for 10 min, and centrifuged for 10 min at 12,000 × g at 4°C. The supernatant was discarded with a micropipette. The pellet was then resuspended in 1 mL of washing solution (0,3 M guanidine hydrochloride in 95% ethanol), incubated for 20 min, and tubes were centrifuged for 5 min at 7500 × g at 4°C after which the supernatant was discarded. This procedure was repeated twice. 2 mL of 100% ethanol was then added, samples were mixed by vortexing and then incubated for 20 min at room temperature (RT). Next, tubes were centrifuged for 5 min at 7500 × g at 4°C and the supernatant was discarded. Protein pellets were air dried for 5-10 min. The pellets were then resuspended in 200 µl of 2x SDS-PAGE sample buffer (20 % Glycerol, 4 % SDS 100 mM, Tris pH 6,8, 0.2 % Bromophenol blue and 100 mM DTT) to solubilize the proteins, pipetted up and down and homogenized with the tissue homogenizer (Retsch MM400 Tissue Lyser). The samples were incubated at 50°C for 10 min in a thermomixer and centrifuged for 10 min at 10,000 × g at 4°C. The resulting supernatant was transferred to new tubes and Nanodrop1000 was used for protein quantification, measuring the absorbance at 280nm. The samples were stored at -20°C.

#### b) *C2C12 cell samples*

Cells were pelleted and directly resuspended in 100 µl of 2x SDS-PAGE sample buffer. To degrade DNA and RNA, cell lysates were incubated with benzonase at room temperature for 10 min. Cell lysates were heated at 50°C for 10 min and centrifuged at maximum speed for 5 min. The supernatant was transferred to a new microcentrifuge tube and to determine protein quantification, Nanodrop1000 was used measuring the absorbance at 280 nm. The samples were stored at -20°C.

### 2.4.2 Western Blot

The proteins under analysis ranged between 25-125kDa and for this reason 10% or 12% polyacrylamide gels were used to separate proteins. Samples were loaded in the gel (approximately 20µg of protein) and then ran in 1x Running Buffer (3,02 g Tris base, 14,42 g Glycine, 1 g SDS in 1 L distilled water) for 1 h at 150 V, using the Mini-PROTEAN® Tetra electrophoresis system (Bio-Rad). Next, a transfer cassette was mounted with the gel and a polyvinylidene fluoride (PVDF) membrane, previously activated with methanol, was added. The Mini Trans-Blot® Cell (Bio-Rad) was used for protein transfer with chilled Transfer Buffer (5.82 g Tris, 2,93 g glycine in 1 L distilled water) for 45 min at 100V. After transfer, to confirm the

quality of protein extracts and verify the loading of the gel, GelCode™ Blue Safe Protein Stain (ThermoFisher Scientific) was used to stain the gel for 1 h. Next, membranes were blocked for 1 h in 5% powdered milk in TBST (20 mM Tris, 150 mM NaCl, 0.1 % Tween20 and distilled water, pH 7.4-7.6), with agitation. Membranes were rinsed 3 times in TBST and incubated with the primary antibody, diluted in 2% bovine serum albumin (BSA) in TBST and 0.02% Sodium Azide overnight at 4°C, with agitation (antibodies and dilutions used are listed in Table S5, Annex). The next day, membranes were incubated with secondary antibodies coupled with horseradish peroxidase (HRP) diluted in 5% powdered milk in TBST for 1 h at RT, after being previously washed in TBST. Membranes were washed 3 times, for 10 min each, in TBST and chemiluminescence was detected using Supersignal™ West Pico Chemiluminescent Substrate HRP (ThermoFisher Scientific). Images were acquired using the Amersham Imager 680 RGB (GE Healthcare).

## 2.5. Immunofluorescence

### 2.5.1 Cell lines

Approximately, 25.000 cells (WT and selected KO clones) were plated in 24-well plates with coverslips and cultured for 48h. Cells were then washed with 1x PBS, fixed in 4% paraformaldehyde for 10 min at RT, washed again with 1x PBS and permeabilized for 5 min in 0,1% Triton. After washing twice with 1X PBS, cells were blocked for 1h at room temperature with blocking solution (1% BSA, 1% goat serum, 0.05% Triton-X100, all in PBS). Cells were then incubated in primary antibodies diluted blocking solution overnight at 4°C. On the following day, cells were incubated in secondary antibodies diluted in blocking solution for 1 h at room temperature and were then washed twice with blocking solution. Cells were counterstained with DAPI (4',6-diamidino-2-phenylindole) for 30 sec, before mounting. Cells on coverslips were removed from the plate, quickly rinsed with water and left drying for 20-30 min. Mounting media (50 mg/ml propyl gallate in PBS: glycerol, 9:1) was used to mount coverslips on slides. Immunofluorescence images were acquired with an Olympus BX60 fluorescence microscope. Primary and secondary antibodies are listed in Table S5 (Annex).

### 3. Results

#### *Lama2*-deficiency alters the *myogenin* pathway in C2C12 cells, and to a lesser extent *in vivo*.

Previous data from the host laboratory showed that disease onset in the *dy<sup>W</sup>* mouse model for LAMA2-CMD occurs between mouse developmental stages E17.5 and E18.5.<sup>20</sup> During the transition between these two stages, a dramatic decrease in the number of Pax7- and myogenin-positive cells was observed<sup>20</sup>, but the mechanisms causing this were not fully explored.<sup>20</sup> To understand if myogenin pathway was altered at the transcriptional level in myoblasts/MuSCs in the absence of *Lama2*, the gene expression of *Myog* (encoding myogenin) and its target genes, *Myh1* and *Tubb6*, was analysed by RT-qPCR. This analysis was performed *in vivo*, through the analysis of epaxial muscles collected from WT and *dy<sup>W</sup>* foetuses at E17.5 (Figure 3.1A) and E18.5 (Figure 3.1B), as well as *in vitro* in regular proliferation medium (PM), using a C2C12 myoblast cell line lacking *Lama2* gene as an *in vitro* model for LAMA2-CMD (Figure 3.1C).

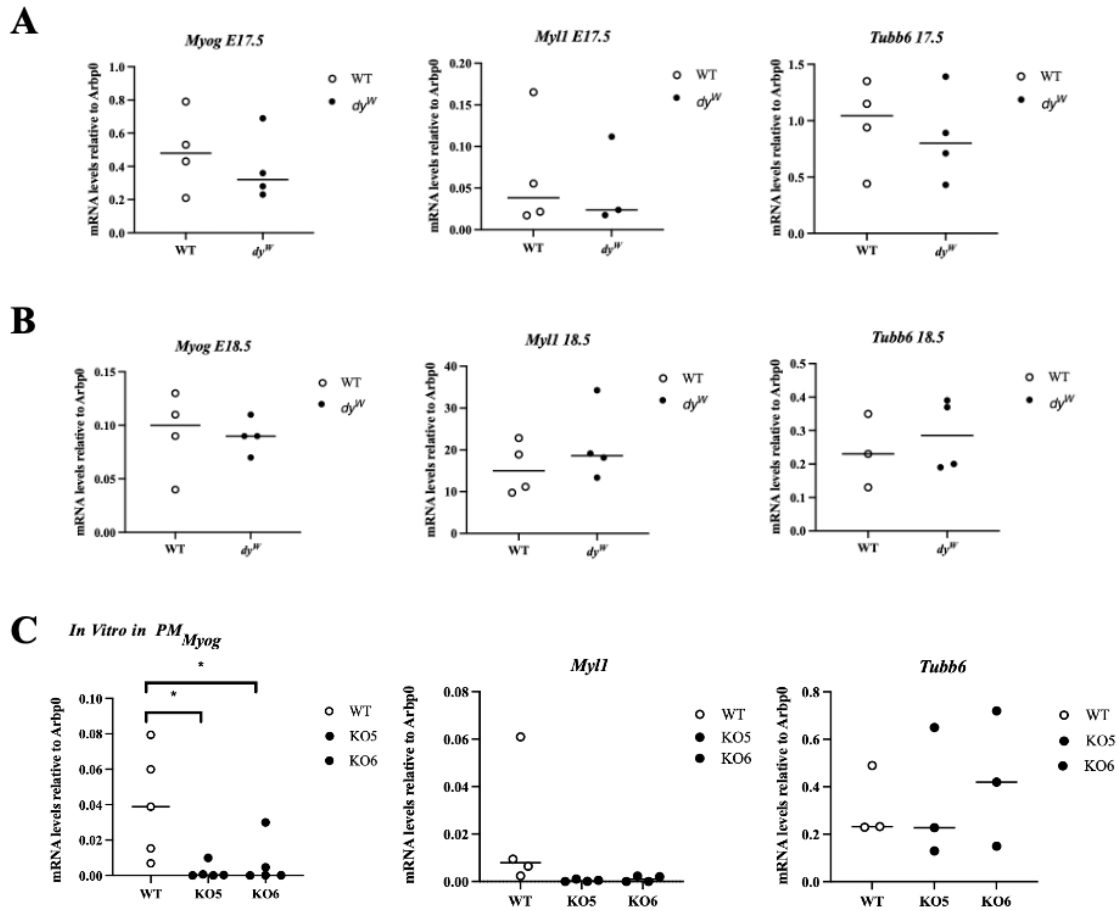


**Figure 3.1: Absence of *Lama2* alters myogenin pathway *in vitro*, and to a lesser extent *in vivo*.** Relative transcript levels of *Myog* and its target genes *Myh1* and *Tubb6* was analysed *in vivo*, in WT and *dy<sup>W</sup>* mice epaxial muscle samples at E17.5 (A) and at E18.5 (B). Transcript levels were normalized with the housekeeping gene *Arbp0*. Each dot represents an individual sample, n=3-4 independent fetuses. *In vivo* statistical analyses were performed by Mann-Whitney non-parametric test. C: mRNA expression levels of *Myog* and its target genes *Myh1* and *Tubb6* was analysed *in vitro* in WT C2C12 cells (WT) and two independent *Lama2* KO C2C12 single cell clones (KO5 and KO6) cultured in proliferation medium (PM). *In vitro* statistical analyses were performed by one-way ANOVA, \* p-value < 0,05. Transcript levels were normalized with the housekeeping gene *Arbp0*. Each dot represents an individual sample, n=3-5 independent experiments. Horizontal lines represent median values.



Regarding the analysis of myogenin (*Myog*) and its target genes *in vivo*, at E17.5 there is a tendency for a decrease, although not significant, in the expression levels of *Myog* and *Tubb6* in *dy<sup>W</sup>* whole muscle samples compared to WT ones (Figure 3.1A). At E18.5, there are no differences in the expression of *Myog* and its target genes (Figure 3.1B). In contrast, in C2C12 cells cultured *in vitro*, the *Myog* expression levels in the C2C12 KO lines was significantly decreased compared to the WT C2C12 cells (Figure 3.1C) (one-way ANOVA test, KO5 \*p-value: 0,0208 and KO6 \*p-value: 0,0237). There is a tendency for a decrease, albeit not significant, in *Myll* expression in C2C12 KO cells (one-way ANOVA test, KO5 \*p-value: 0.2021 and KO6 \*p-value: 0,2207) compared to WT cells and no significant differences in *Tubb6* (one-way ANOVA test, KO5 \*p-value: 0,9938 and KO6 \*p-value: 0,8042) (Figure 3.1C). Overall, these data suggests that absence of *Lama2* reduces *Myog* expression in C2C12 cells cultured in PM and there is a tendency in the same direction in whole muscle samples at E17.5. particularly in myoblasts and MuSCs, and consequently in its target genes, *Myll* and *Tubb6*.

### **Lama2-deficiency alters Nfix expression and Myf5 localization in C2C12 cells.**

MuSCs at fetal stages of development activate the expression of Nfix downstream of Pax7.<sup>27</sup> When these cells enter the myogenic differentiation program, they express MRFs and finally myogenin commits these cells to form fusion-competent myoblasts.<sup>21</sup> It has previously been described that Nfix plays a dual role in myogenesis, being responsible for the inhibition of genes expressed during embryonic (primary) myogenesis, such as the slow myosin heavy chain (*MyHC-slow*), and for the activation of genes characteristic of fetal myogenesis such as Enolase- $\beta$  (*Eno3*) and muscle creatine kinase (*Ckm*), downstream targets of the Nfix pathway.<sup>27</sup> To investigate how *Lama2*-deficiency impacts fetal myogenesis, most specifically, how it impacts *Nfix* and its target genes *Eno3* and *Ckm* at E17.5 and E18.5, we analyzed the expression of these genes by RT-qPCR, *in vivo* and *in vitro* (Figure 3.2). Since *in vitro*, *Nfix* gene expression levels were not conclusive (RT-qPCR melting curves were inadequate), Nfix protein expression levels were analyzed by immunofluorescence and Western Blot, in C2C12 myoblast cell lines (Figure 3.2C and D) and gene expression levels of Nfix target gene *Eno3* were detected by RT-qPCR (Figure 3.2E).<sup>27</sup>

At E17.5, gene expression levels of *Nfix* and its target gene *Eno3* showed a slightly tendency to be increased in *dy<sup>W</sup>* epaxial muscle samples, compared to the WT samples (Figure 3.2A). In contrast, at E18.5 *Nfix* and *Ckm* gene expression levels showed a slightly tendency to be decreased in *dy<sup>W</sup>* epaxial muscle samples compared to the WT, while *Eno3* did not present differences between *dy<sup>W</sup>* and WT (Figure 3.2B).

The mRNA expression in C2C12 myoblast cell lines cultured in proliferation medium for *Nfix* and *Ckm* were inconclusive, it will be necessary in the future to repeat the analysis with more specific primers. As *Nfix* expression was only detected *in vivo*, with no significant differences, immunofluorescence and Western Blot were used to investigate if Nfix protein levels were altered in the absence of *Lama2*, *in vitro*. The immunofluorescence results showed a significant increase of the number of Nfix-positive cells in C2C12 *Lama2* KO cultures compared to WT (one-way ANOVA test, \*\*\*\* p-value:0,0001) (Figure 3.2C, C'). In support of this result, Western Blot analysis showed an increase in total Nfix protein levels in KO cells compared to WT cells (Figure 3.2D, D'). However, the expression of the Nfix target gene, *Eno3* was similar between C2C12 WT and KO *Lama2* myoblasts (Figure 3.2E).

Considering that Pax7 is thought to induce Nfix expression in fetal development<sup>27</sup>, next it was addressed the expression of Pax7 and the MRFs in WT and KO C2C12 cells cultured in proliferation medium and, in the case of Pax7, also in whole muscle samples. Immunolocalization of Pax7 in C2C12 cells showed very low expression in WT and KO6 C2C12 cells, but interestingly cells of the KO5 clone displayed clear nuclear Pax7 staining (Figure 3.3A). Quantification of the percentage of Pax7-positive cells demonstrated that significantly more KO5 cells express Pax7 compared to both WT and KO6 C2C12 cells (one-way ANOVA test, \*\*\*p-value: 0,0002) (Figure 3.3A'). RT-qPCR analysis of *Pax7* gene expression in these cells also

show a higher expression in clone KO5 compared to WT and KO6 (Figure 3.3B). This result suggests that somehow this clone, C2C12 *Lama2* single cell KO5, is in an earlier period of development compared with the WT and the C2C12 *Lama2* single cell clone KO6.

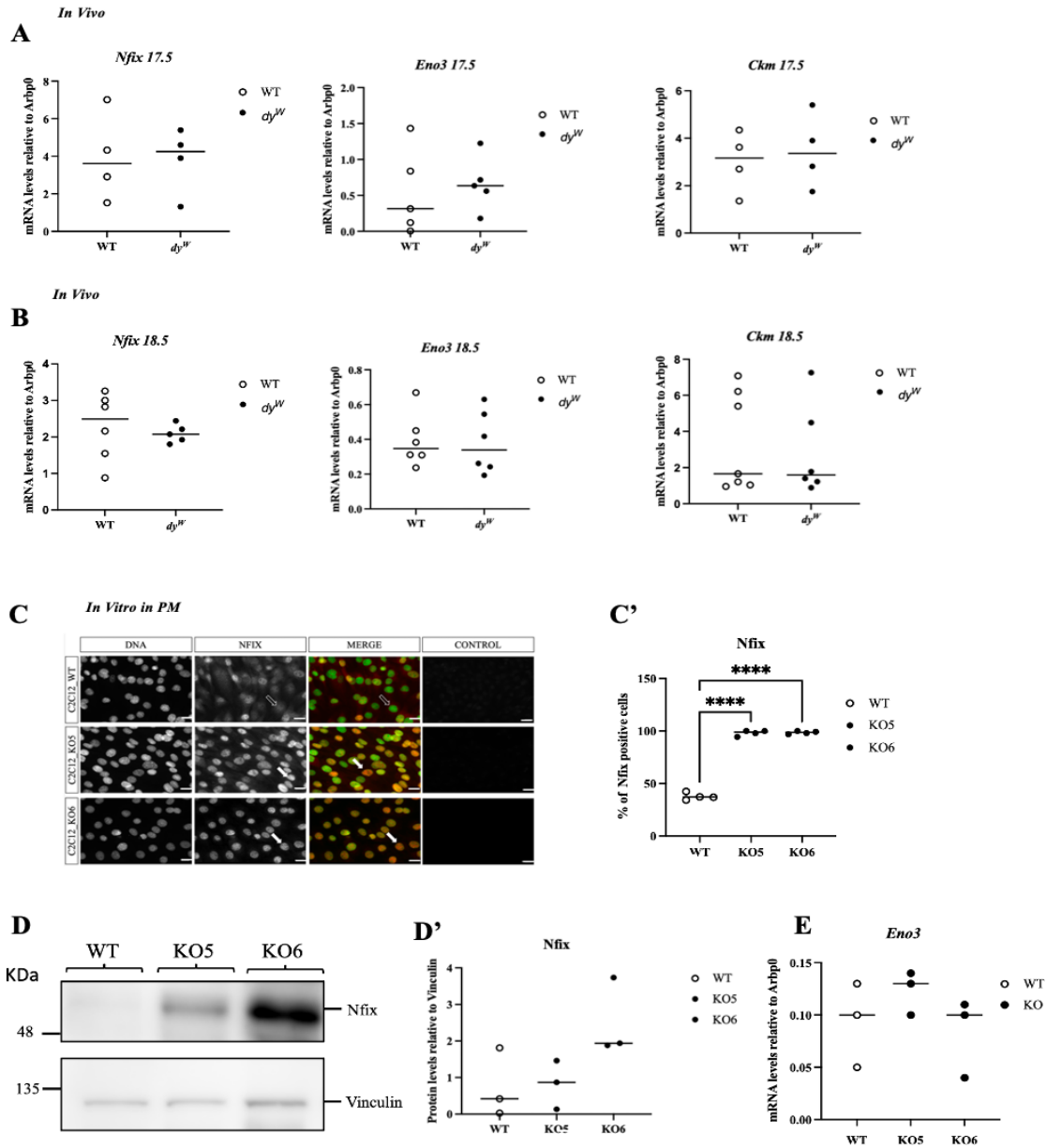


**Figure 3.2: Absence of *Lama2* alters *Nfix* pathway *in vivo* and *in vitro*.** Relative transcript levels of *Nfix* and its target genes *Eno3* and *Ckm*. **A:** *In vivo*, in WT and *dy<sup>W</sup>* mice epaxial muscle samples at E17.5 and **B:** at E18.5. *In vivo* statistical analyses were performed by Mann-Whitney test. Each dot represents an individual sample, n=4-6 independent fetuses **C:** *In vitro*, Representative images of immunofluorescence labelling for *Nfix* (red) and DNA staining (green) in WT C2C12 cells (WT) and *Lama2* KO C2C12 cells (KO) cultures in proliferation medium (PM). **C'**: quantification of the percentage of *Nfix* positive cells in the culture. n=3 independent experiments. Scale bars: 50  $\mu$ m. Control refers to cells stained only with the secondary antibody staining. p-values were calculated with one-way ANOVA, \*\*\*\*< 0,0001. **D:** Western Blot (WB) for *Nfix* protein in WT C2C12 cells (WT) and two single cell clones of *Lama2* KO C2C12 cells (KO5 and KO6). Vinculin was used as loading control. **D'**: quantification of *Nfix* protein levels as detected by WB. Statistical analysis was performed with one-way ANOVA test. **E:** Relative transcript levels of *Eno3* in WT C2C12 cells (WT) and two single cell clones of *Lama2* KO C2C12 cells (KO5 and KO6). Statistical analysis was performed with one-way ANOVA test. Transcript levels were normalized with the housekeeping gene *Arbp0*. Each dot represents an individual sample, n=3 independent experiments. Horizontal lines represent median values.

To further understand if myogenesis is compromised by the absence *Lama2* in C2C12 cells, we performed immunofluorescence for the MRF Myf5. C2C12 *Lama2* KO cultures have a significantly higher percentage of Myf5-positive cells compared to the WT cultures (KO5 p-value: 0,0229 and KO6 p-value: 0,0152, Figure 3.3C'). Interestingly, analysis of the immunofluorescence images reveal that whereas Myf5 protein is primarily nuclear in WT C2C12 cells, it is mostly cytoplasmic in the KO lines (Two-way ANOVA test, \*\*\*\* p-value<0,0001) (Figure 3.3 C, C'). The data obtained suggests that in the absence of *Lama2*, Myf5 protein does not enter the nucleus as happens in the WT cells, but is retained in the cytoplasm.

The protein expression of MyoD, another MRF involved in the commitment of myoblasts to myogenesis, was analysed in Western Blot in C2C12 WT and *Lama2* KO cell lines, cultured in PM. The data obtained suggests that, although not significant, MyoD tends to be increased in *Lama2* KO myoblasts compared to the WT (Figure 3.3D, D').

Overall, these results suggest that there are no significant differences in the expression of *Nfix* and its target genes when comparing whole *dy<sup>W</sup>* and WT epaxial muscles. However, in C2C12 cells cultured *in vitro* in proliferation medium, the percentage of cells with nuclear Nfix protein expression is significantly increased in C2C12 *Lama2* KO myoblasts compared to the WT. This finding, together with the observation that the Myf5 is retained in the cytoplasm in *Lama2* KO cells, and that MyoD levels are slightly altered, suggests a defect in myoblast differentiation.

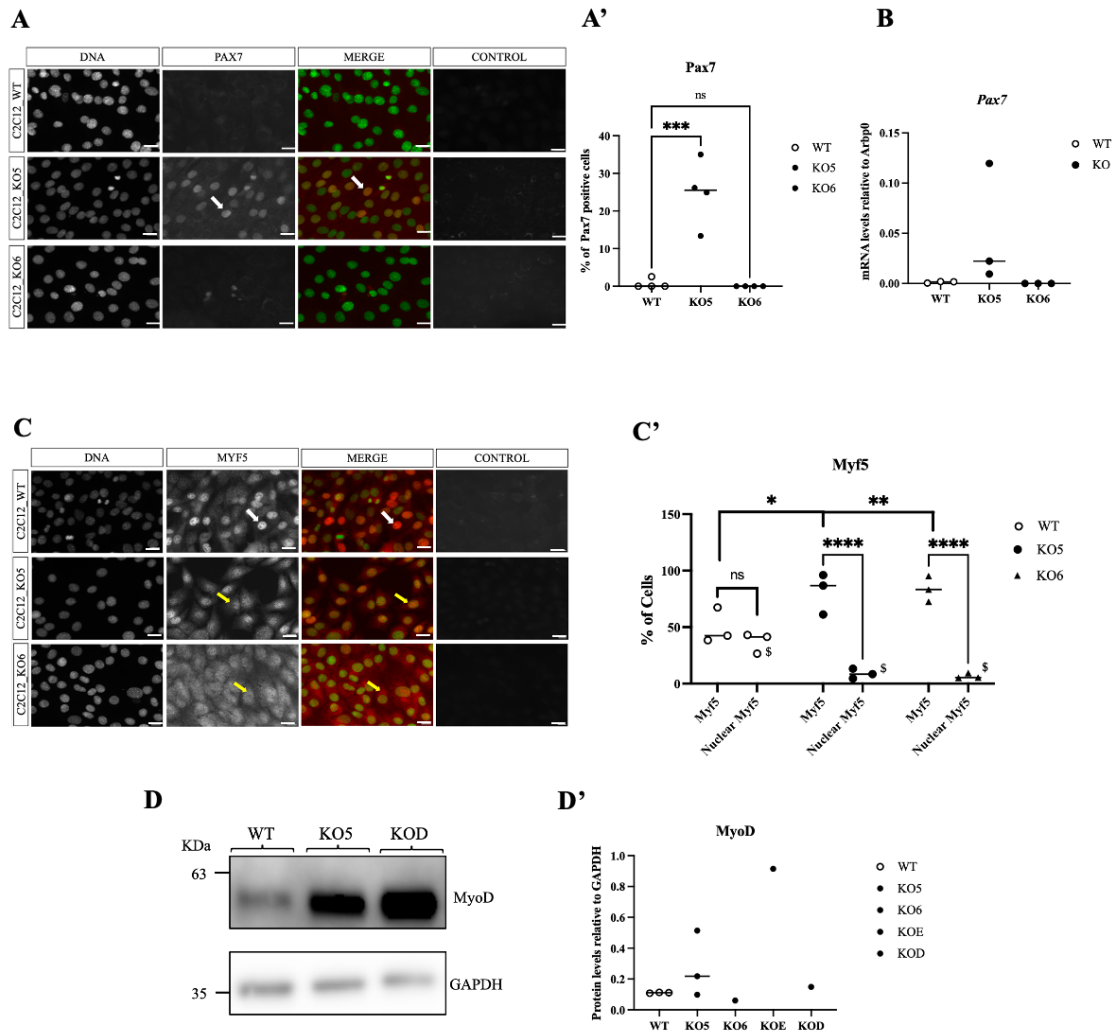
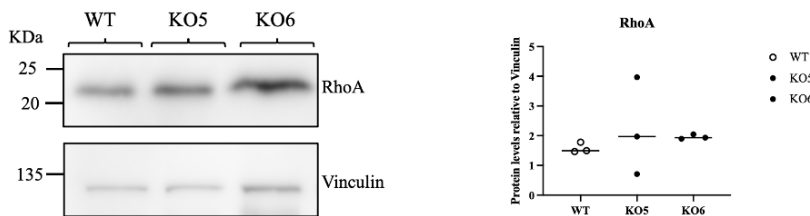


**Figure 3.3: Impact of *Lama2*-deficiency in Pax7 expression and Myf5 localization in C2C12 cells.** **A:** Representative images of immunofluorescence labelling for Pax7 (red) and DNA staining (green); **A':** quantification of percentage of Pax7-positive cells. Relative transcript levels of *Pax7* in WT C2C12 cells (WT) and two single cell clones of *Lama2* KO C2C12 cells (KO5 and KO6), cultured in proliferation medium (PM). Statistical analysis was performed with one-way ANOVA test. **B:** RT-qPCR analysis of *Pax7* expression. Transcript levels were normalized with the housekeeping gene *Arbp0*. Each dot represents an individual sample, n=3 independent experiments. Horizontal lines represent median values. **C** Representative images of immunofluorescence labelling for Myf5 (red) and DNA staining (green) in WT C2C12 cells (WT) and *Lama2* KO C2C12 cells (KO), cultured in PM. Full white arrows indicate high expression in the nucleus, outlined arrows indicate low expression in the nucleus and yellow arrows indicate cytoplasmatic expression. **C':** Quantification of the percentage of Myf5-positive cells (Myf5) and the percentage of cells with nuclear Myf5 staining (nuclear Myf5). Two independent *Lama2* KO single cell clones are represented (KO5 and KO6). n=3 independent experiments. Scale bars: 50  $\mu$ m. p-values were calculated with one-way ANOVA, p-values: \* <0,05 \*\*< 0,01 \*\*\*\*< 0,0002, \*\*\*\*\*< 0,0001. \$ indicate significance in nuclear Myf5. **D:** Analysis of MyoD by Western Blot in WT C2C12 cells and four *Lama2* KO C2C12 cell lines established from four independent single cell clones (KO5, KO6, KOE and KOD), cultured in PM. GAPDH was used as a loading control. MyoD protein expression level normalized to GAPDH. **D':** Quantifications are shown on the right. n=3.

## Effect of *Lama2*-deficiency on RhoA and Erk pathways in C2C12 cells

RhoA and ROCK repress Erk kinase activity, which promotes JunB and Nfix expression.<sup>26</sup> To investigate how *Lama2* deletion impacts RhoA and Erk signalling, protein expression levels of both were analysed by Western Blot using the WT and *Lama2* KO C2C12 cell lines cultured in PM (Figure 3.4). The data obtained suggests that there is a tendency for RhoA to be increased in *Lama2* KO cells, compared to WT (Figure 3.4A). Although not significant, P-Erk1 and P-Erk2 present a tendency to be increased in *Lama2* KO cells, compared to the WT (Figure 3.4B). Erk levels did not differ between *Lama2* KO and WT cells. Globally, this data suggests that there is a tendency for RhoA and P-Erk to be increased in *Lama2* KO cell lines compared to WT. Therefore, future experiments should validate protein expression levels of Erk and P-Erk *in vivo*.

**A**



**B**

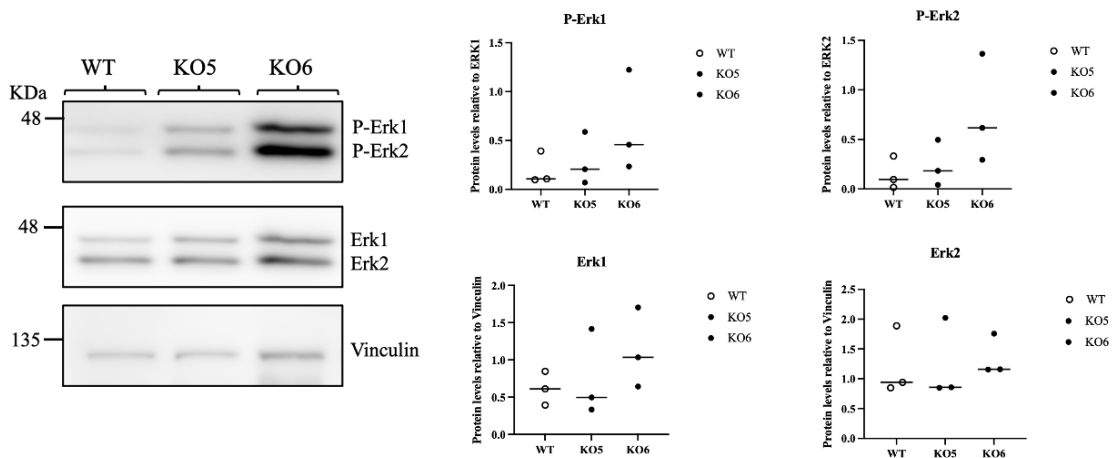


**Figure 3.4: *Lama2*-deficiency and RhoA and Erk pathways *in vitro*.** **A:** Analysis of RhoA by Western Blot in WT C2C12 cells (WT) and two single cell clones of *Lama2* KO C2C12 cells (KO5 and KO6), cultured in proliferation medium (PM). n=3 independent experiments. **B:** Analysis of P-Erk and Erk by Western Blot in WT C2C12 cells (WT) and two single cell clones of *Lama2* KO C2C12 cells (KO5 and KO6), cultured in PM. n=3. Vinculin was used as loading control. RhoA and Erk proteins expression levels were normalized to vinculin and P-Erk proteins expression levels were normalized to Erk. Quantifications are shown on the right. Statistical analysis was performed by one-way ANOVA.

### Effect of *Lama2*-deficiency on *Akirin1* and *Notch1* expression

Studies have demonstrated that Notch signalling not only plays a role in the maintenance of MuSCs, but also ensures proper homing of satellite cells to their niche.<sup>53</sup> Specifically, at fetal stages of development Notch signalling has been described as inducing Pax7 expression and inhibiting MyoD and Myogenin, leading to an inhibition of myoblasts commitment and inducing MuSCs proliferation.<sup>53</sup> To understand if *Notch1* gene expression is altered in the absence of *Lama2*, RT-qPCR was performed in epaxial muscle samples from *dy<sup>W</sup>* and WT mice and in C2C12 WT and *Lama2* KO cell lines, cultured in proliferation medium. The data obtained suggests that there is a tendency for an increase, albeit not statistically significant, in *Notch1* gene expression in *Lama2* KO myoblasts compared to WT (Figure 3.5A). In whole muscle samples collected at E17.5 *Notch1* gene expression is slightly, but not significantly, increased in the *dy<sup>W</sup>* epaxial muscle samples compared to the WT (Figure 3.5B), while there are no differences in Notch expression in *dy<sup>W</sup>* epaxial muscle samples compared to WT at E18.5 (Figure 3.5C).

Studies using myogenic cell lines showed that Myostatin inhibits myoblasts proliferation, and impacts myoblasts differentiation.<sup>32</sup> We thus assessed the expression of *Akirin1*, a target gene of *Myostatin*, by RT-qPCR. However, the data obtained suggests that there are no differences in *Akirin1* gene expression levels between epaxial muscle samples from *dy<sup>W</sup>* and WT mice, nor between WT and *Lama2* KO cell lines (Figure 3.5B-C).

*Notch1* gene expression levels showed a tendency to be increased in *Lama2* KO C2C12 cells compared to WT and at E17.5 in *dy<sup>W</sup>* epaxial muscle samples compared to the WT, which is in accordance with previous studies.<sup>53</sup> However, *Akirin1* gene expression levels do not present differences between *Lama2* KO myoblasts compared to WT nor between *dy<sup>W</sup>* epaxial muscle samples compared to the WT. However, more studies are necessary before excluding the Myostatin pathway as a player in *Lama2*-deficiency.

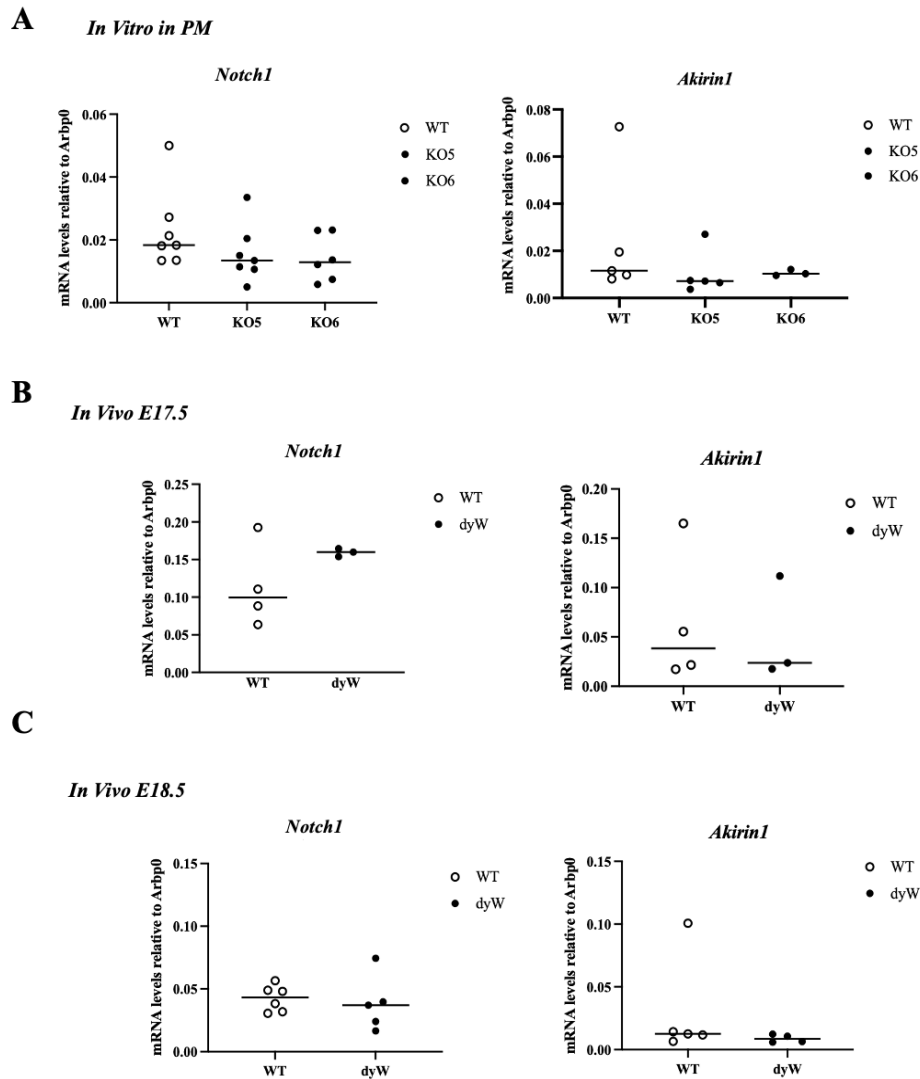


**Figure 3.5: Notch and Myostatin pathways in the absence of *Lama2* in C2C12 cells and fetal muscle samples.** **A:** Relative transcript levels of *Notch1* and *Akirin1* in WT C2C12 cells and two single cell clones of *Lama2* KO C2C12 cells (KO5 and KO6), cultured in PM; and in WT and dyW epaxial muscle samples at E17.5 (**B**) and at E18.5 (**C**). Transcript levels were normalized to the housekeeping gene *Arbp0*. Each dot represents an individual sample, n=3-7, independent experiments. Horizontal lines represent median values. Statistical analysis was performed using a one-way ANOVA (C2C12 cells) and Mann-Whitney tests (fetal muscle samples).

### **Lama2-deficiency impacts myoblasts differentiation of C2C12 cells in vitro**

To investigate if the absence of *Lama2* impacts myoblast differentiation and fusion into myotubes, C2C12 *Lama2* KO and WT myoblasts were differentiated *in vitro*, and their differentiation was followed over time (Figure 3.6A). The data obtained showed that C2C12 *Lama2* KO myoblasts took longer to elongate and align and did not fuse within the time frame of the experiment. At day five is possible to see numerous aligned myotubes in the WT C2C12 cell cultures. *Lama2* KO C2C12 myoblasts were delayed in elongation and alignment compared to WT cells, but by day 5, they were close together and aligned to a certain extent; however, no myotubes were present (Figure 3.6A). To further validate these results, an immunofluorescence labeling for myosin heavy chain to detect myotubes, and fibronectin was performed (Figure 3.5B). Data showed positive staining for myosin heavy chain in WT myotubes, but in the *Lama2* KO cultures myosin heavy chain staining was practically absent (Figure 3.5B). Immunostaining for fibronectin shows labeling in both WT and *Lama2* KO cell lines (Figure 3.6C). However, close inspection of the images indicates that the C2C12 KO cell lines present a tendency to express more Fibronectin than the WT cells (Figure 3.6C), establishing a Fibronectin network resembling a pericellular matrix. This may indicate a compensatory behaviour in absence of *Lama2*.



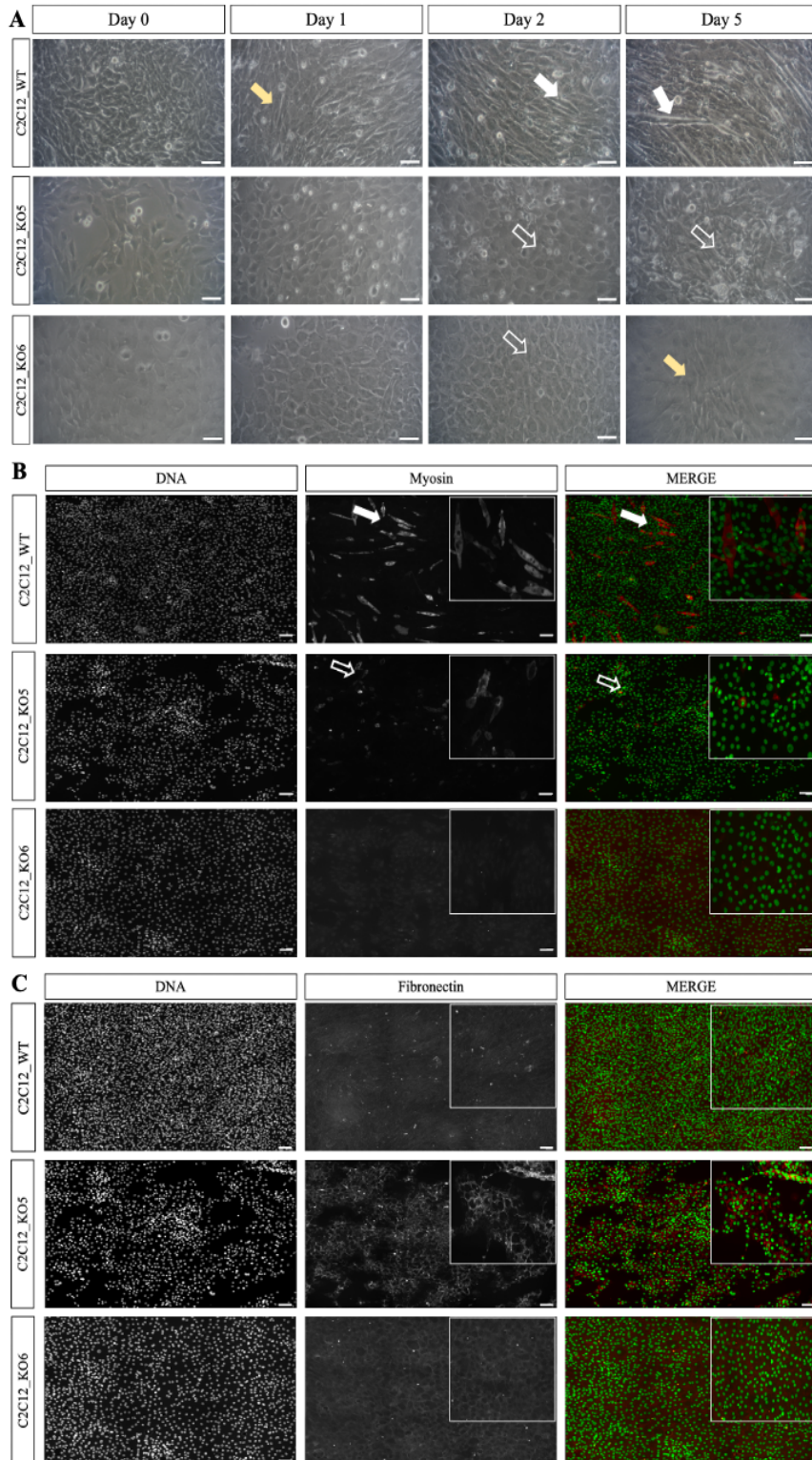


**Figure 3.6 Deletion of *Lama2* delays myotube formation.** **A:** Phase-contrast images of C2C12 cell cultures in proliferation medium (PM) (day 0) and then after 1 (when differentiation media was added), 2 and 5 days in differentiation medium. WT cells displayed myotubes on day 2 and 5, while *Lama2* KO cells do not. Full white arrows indicate myotubes, full yellow arrows indicate myoblast elongation and alignment, and open arrows indicate the absence of myotubes. Scale bars: 50  $\mu\text{m}$ . **B:** Nuclear staining (DAPI in green) and immunofluorescence labelling for Myosin heavy chain (red) in WT cells (WT) and *Lama2* KO cells. Full white arrows indicate myotubes, open arrows point to rare incipient myotubes formation in the KO cultures. **C:** Nuclear staining (DAPI in green) and immunofluorescence labelling for Fibronectin (red) in WT cells (WT) and *Lama2* KO C2C12 cells. Representative images are shown. n=3 independent



**Jak-Stat3 pathway is altered in the context of *Lama2*-deficiency in C2C12 cells, and to a lesser extent *in vivo*.**

Myoblasts differentiation can be induced or inhibited by the Jak-Stat pathway.<sup>34</sup> The host laboratory previously showed that P-Stat3 was significantly increased in *dy<sup>W</sup>* fetal muscles on E17.5, suggesting that *Lama2*-deficiency is marked by the overactivation of Stat3 signal.<sup>20</sup> To investigate if C2C12 cells lacking *Lama2* also present overactivation of Jak-Stat pathway, a Western Blot was performed to detect P-Stat3 and Stat3 proteins in the C2C12 WT and *Lama2* KO cell lines cultured in proliferation medium (Figure 3.7). In addition, the same analysis was also performed with epaxial muscles not only from stage E17.5, but also E18.5 (Figure 3.7B, C).<sup>20</sup> The data obtained suggests a significant increase of P-Stat3 in *Lama2* KO myoblasts cultured *in vitro* compared to the WT (one-way ANOVA test, \* p-value:0,0340), while the total Stat3 levels remain unaltered (Figure 3.7A). *In vivo*, at E17.5, P-Stat3 protein showed a tendency to be increased in *dy<sup>W</sup>* muscle samples compared to the WT ones, which is in accordance with previously published data<sup>20</sup> (Figure 3.7B). However, data obtained suggest that there are no differences in P-Stat3 and Stat3 proteins expression in E18.5 *dy<sup>W</sup>* muscle samples compared to the WT (Figure 3.7C). Nevertheless, overall, these data suggest that P-Stat3 may be increased in the absence of *Lama2* and this is particularly evident in the C2C12 cells.

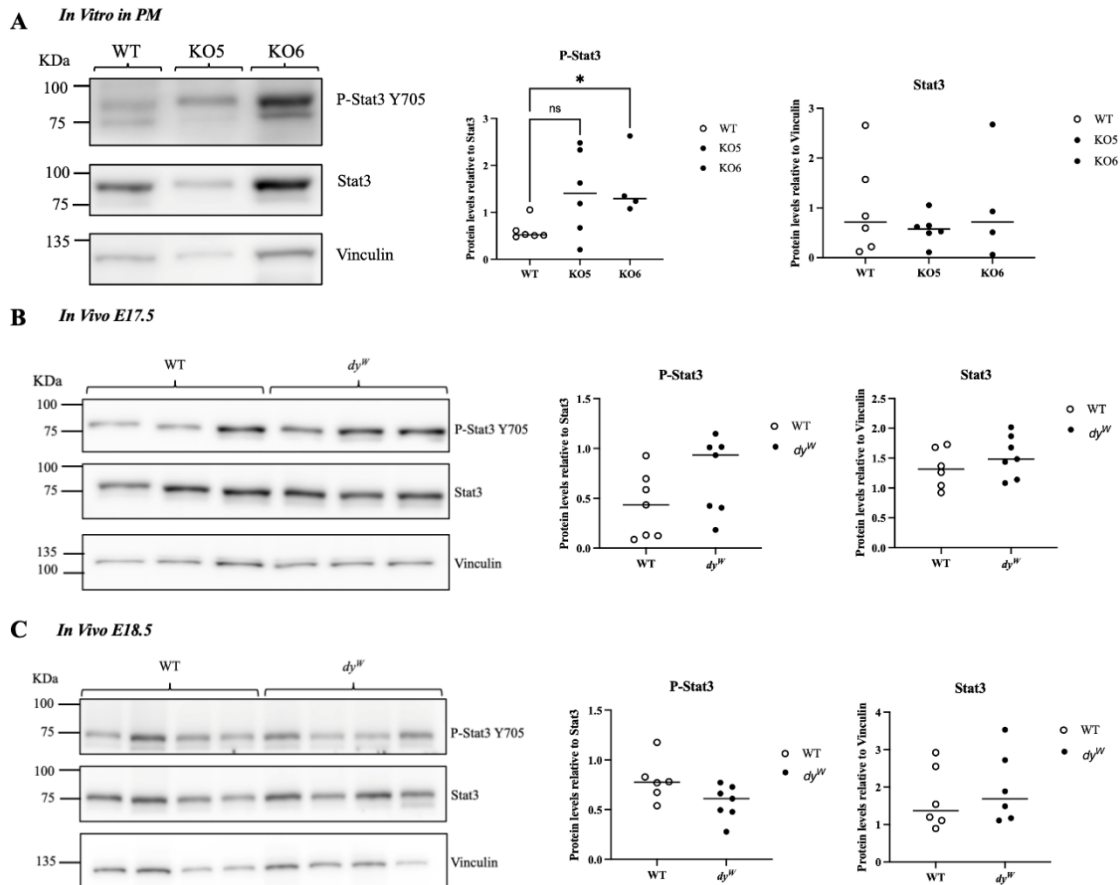


**Figure 3.7: Jak-Stat pathway in the context of *Lama2*-deficiency in C2C12 cells and fetal muscle samples.** Analysis of P-Stat3 (Y705, Tyrosine 705) and Stat3 by Western Blot in: **A:** WT C2C12 cells (WT) and two single cell clones of *Lama2* KO C2C12 cells (KO5 and KO6), cultured in proliferation medium (PM), n=6 independent experiments; **B:** WT and *dy<sup>W</sup>* muscle samples at E17.5 n=6-7 independent fetuses; and **C:** in WT and *dy<sup>W</sup>* muscle samples at E18.5, n=6-7 independent fetuses. Vinculin was used as a loading control. Protein expression of P-Stat3 was normalized to Stat3 and Stat3 protein expression was normalized to Vinculin. Quantifications are shown on the right. Statistical analysis was performed by one-way ANOVA, \*p<0,05.

## Lama2-deficiency impacts FAK signaling pathway *in vitro* and *in vivo*

FAK, activated downstream of integrin signalling, has been described as an important factor for myoblasts differentiation through MyoD activation and is necessary for myotube formation by activating Cdc42 that allows myoblasts fusion.<sup>38</sup> To explore whether *Lama2*-deficiency impacts the FAK pathway, P-FAK and total FAK were analysed by Western Blot in C2C12 WT and *Lama2* KO cell lines cultured in PM and in epaxial muscles from WT and *dy<sup>W</sup>* fetuses at E17.5 and E18.5 (Figure 3.8). The data obtained suggests a slight tendency for P-FAK to be increased in *Lama2* KO myoblasts compared to WT, although no differences were observed in FAK protein expression (Figure 3.8A). *In vivo*, there was a significant increase of P-FAK protein levels in E17.5 *dy<sup>W</sup>* muscle samples (t-test, \* p-value: 0,018), compared to the WT, while total FAK remained unchanged (Figure 3.8B). In contrast, at E18.5 there was a tendency for P-FAK to be decreased and a marked tendency for total FAK to be increased in *dy<sup>W</sup>* muscle samples (t-test, p-value: 0,081), compared to the WT (Figure 3.8C). These data suggest that P-FAK may play a role in *Lama2* deficiency, but more studies are needed to confirm these preliminary results.

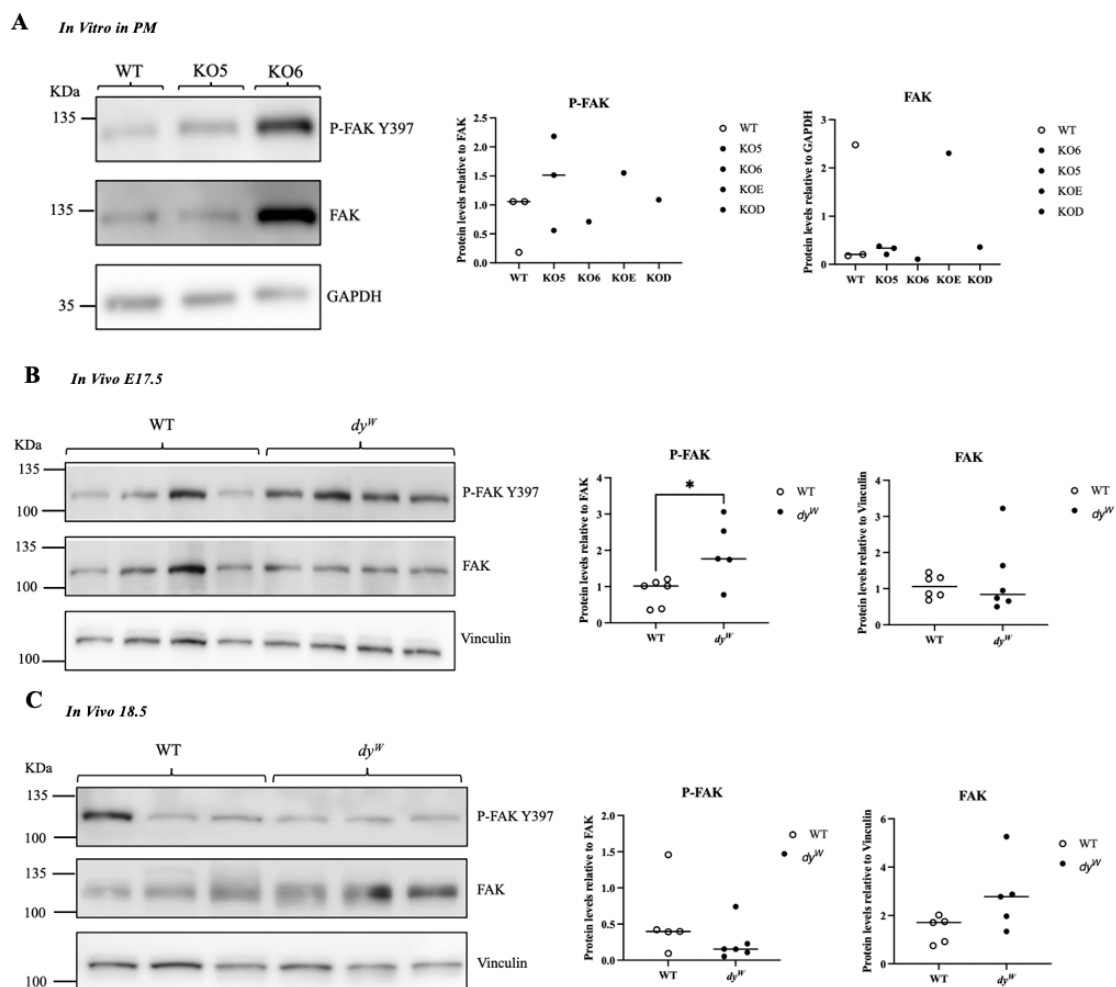


**Figure 3.8: *Lama2*-deficiency and FAK pathway *in vitro* and *in vivo*.** Analysis of P-FAK (Y397, Tyrosine 397) by Western Blot in: **A:** WT C2C12 cells (WT) and four single cell clones of *Lama2* KO C2C12 cells (KO5, KO6, KOE and KOD), cultured in proliferation medium (PM), n=3 independent experiments. *In vitro*, statistical analysis was performed by one-way ANOVA. **B:** *dy<sup>W</sup>* and WT muscle samples at E17.5 n=5 independent fetuses; and **C:** in *dy<sup>W</sup>* and WT muscle samples at E18.5, n=5 independent fetuses. Vinculin was used as a loading control. Protein expression of P-FAK was normalized to FAK and FAK protein expression was normalized to Vinculin. Quantifications are shown on the right. *In vivo*, statistical analysis was performed by t-test, \*p<0,05.

## Impact of *LAMA2* absence in cancer cells

The results obtained above using two models of *Lama2*-deficiency, namely *Lama2* KO C2C12 cells and muscles from *dy<sup>w</sup>* fetuses, showed that *Lama2*-deficiency impacts a number of signaling pathways important for myoblast differentiation. The next step was to try to understand whether *LAMA2*-deficiency has an impact on these same pathways in other diseases, more specifically in cancer. The ECM composition around cancer cells is crucial for proliferation and evasion.<sup>54</sup> Thus, we investigated the impact of *LAMA2*-deficiency in two cancer cell lines a melanoma (A375) and colorectal (HCT116). Recent studies demonstrated that *LAMA2* gene is associated with melanoma metastasis, being involved in cell adhesion and ECM-receptor interaction<sup>45</sup> and has been described as a methylation target in colorectal cancer.<sup>55</sup>

Besides its impact in myoblasts differentiation, Nfix has been shown to play a significant role in different types of cancer.<sup>25</sup> To determine if Nfix is affected in cancer cells lacking *LAMA2*, Nfix was analysed by immunofluorescence (Figure 3.9A). Data obtained suggests that there are no differences between melanoma WT and KO cancer cell lines (the pool of *LAMA2* KO cells and the *LAMA2* KOF single cell clone).

$\alpha$ -Enolase (*ENO1*), a glycolytic enzyme and a multifunctional oncoprotein present on the cell surface and in the cytoplasm, is involved in carcinogenesis and contributes to seven out of the 10 “hallmarks of cancer”, including leading to ECM degradation that induces angiogenesis and activates invasion and metastasis.<sup>56</sup> To determine whether the absence of *LAMA2* impacts cancer cells, RT-qPCR was performed to analyse the gene expression levels of *ENO1* in melanoma (A375) and colorectal (HCT) WT and KO cancer cell lines. First RT-qPCR was used to confirm that *LAMA2* expression was reduced in the *LAMA2* KO melanoma and colorectal cancer cell lines (Figure 3.9A-B). The data on *ENO1* gene expression levels in the *LAMA2* KO melanoma cell lines suggests a tendency to be decreased, compared to the WT (Figure 3.9B), whereas there is a tendency for an increase in *ENO1* in the KO colorectal cancer cell lines compared to WT (Figure 3.9C).

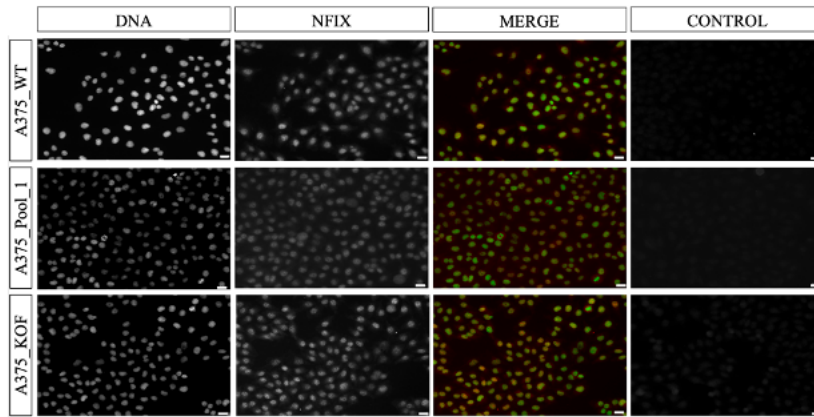
The NOTCH signalling pathway is a regulator of self-renewal and differentiation in several tissues and cell types, its hyperactivation has been implicated as oncogenic in several cancers including breast cancer and T-cell acute lymphoblastic leukaemia.<sup>57</sup> To investigate if *NOTCH1* expression was impacted by the absence of *LAMA2*, RT-qPCR was performed to analyse *NOTCH1* gene expression levels in melanoma (A375) and colorectal (HCT) WT and *LAMA2* KO cancer cell lines. There are no differences in *NOTCH1* gene expression levels in the *LAMA2* KO melanoma cell lines, compared to the WT (Figure 3.9B), while the data obtained suggest a tendency for an increase in *NOTCH* gene expression levels in *LAMA2* KO colorectal cancer cell lines compared to WT (Figure 3.9C).

Taking into account the previously published overactivation of Stat3 in the context of *LAMA2*-CMD<sup>20</sup> and the data obtained in Figure 3.6, the impact of *LAMA2*-deficiency on STAT3 activation in the context of cancer was investigated (Figure 3.9D). For that P-STAT3 levels were analyzed by Western Blot in WT and *LAMA2* KO (KO2, KO3 and KO5) colorectal cancer cell lines. Data obtained suggests that there is tendency for an increase of STAT3 and P-STAT3 in colorectal KO cells compared to WT ones.

Overall, our data suggest that the absence of *LAMA2* may impact *ENO1* expression in melanoma and *ENO1* and *NOTCH* expression in colorectal cancer. Moreover, we find that STAT3 activation may be increase upon *LAMA2*-deficiency in colorectal cancer cell lines.

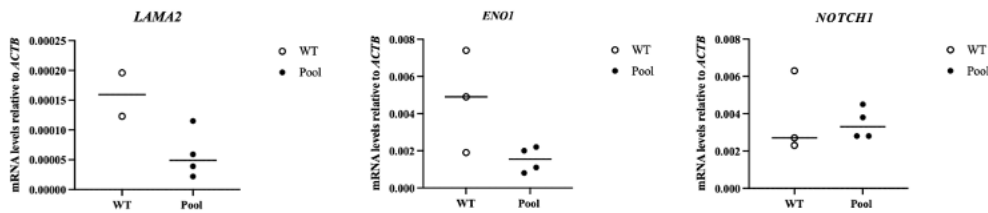
**A**

*Melanoma (A375)*



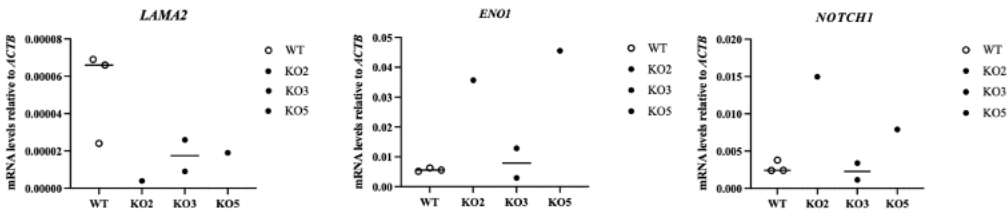
**B**

*Melanoma (A375)*



**C**

*Colorectal (HCT)*



**D**

*Colorectal (HCT)*

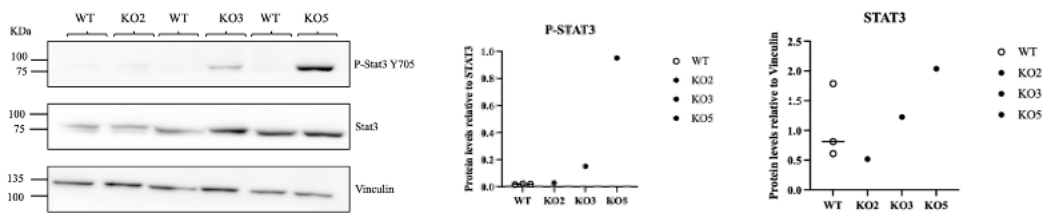


**Figure 3.9: Impact of *LAMA2*-deficiency in melanoma and colorectal cancer cells.** **A:** immunofluorescence labelling for Nfix (green) in melanoma (A375) WT, pool of KO clones (Pool1) and *LAMA2* KO single clone (KOF) cancer cell lines n=1 independent experiment. Scale bars: 50  $\mu$ m. **B:** relative transcript levels of *LAMA2*, *ENO1* and *NOTCH1* in melanoma (A375) WT, and *LAMA2* KO cell lines. **C:** relative transcript levels of *LAMA2*, *ENO1* and *NOTCH1* in colorectal (HCT) WT and KO single clones (KO2, KO3, KO5) cancer cell lines. Statistical analyses were performed by Student's t-test. Transcript levels were normalized with the housekeeping gene *ACTB*. Each dot represents an individual sample, n=3-7, independent experiments. Horizontal lines represent median values. **D:** Analysis of P-STAT3 (tyrosine 705, Y705) by Western Blot in colorectal (HCT) WT and KO single clones (KO2, KO3, KO5) cancer cell lines. Vinculin was used as loading control. STAT3 protein expression was normalized to vinculin, and P-STAT3 was normalized to STAT3. Quantifications are shown on the right, n=1-3 independent experiments per cell line. Statistical analysis was performed by one-way ANOVA.

#### 4. Discussion

LAMA2-CMD is the most common congenital muscular dystrophy and is triggered by mutations in the *LAMA2* gene, codifying the  $\alpha 2$  chain of laminin 211.<sup>41</sup> The onset of the disease is likely to occur *in utero*, as shown by the host laboratory in a mouse model for human LAMA2-CMD (*dy<sup>W</sup>*).<sup>20</sup> This onset occurs between mouse developmental stages E17.5 and E18.5 and is characterized by a dramatic drop in Pax7- and myogenin-positive cells within *dy<sup>W</sup>* muscles<sup>20</sup>. These alteration could impact several aspects of MuSCs and myoblasts development including their ability to differentiate. In this project, by performing a differentiation assay using the *in vitro* model for LAMA2-CMD, it was shown that *Lama2* KO C2C12 cells do not form myotubes after five days in differentiation medium, while WT C2C12 cells form myotubes in two days (Figure 3.6A and B), supporting the idea that *Lama2*-deficiency impairs myoblast differentiation.

To dissect out which pathways are altering myoblast differentiation in the absence of *Lama2* both *in vivo* and in the C2C12 model *in vitro*, the expression of *Pax7*, *Myog* and myogenin target genes *Myll* and *Tubb6* was assessed in both the C2C12 cell line model and *in vivo* (Figure 3.1). Expression of *Myog* was significantly decreased in *Lama2*-deficient C2C12 cells *in vitro* compared to WT (Figure 3.1C). *Myog*, *Myll* and *Tubb6* expression levels showed a tendency to be decreased in C2C12 cells *in vitro* and in E17.5 *dy<sup>W</sup>* epaxial muscle samples, compared to WT, although at E18.5 the expression of these genes showed a slight tendency to be increased (Figure 3.1). Since myogenin is essential for myoblasts differentiation into myocytes that will fuse to form myotubes<sup>17</sup>, these results indicate that in absence of *Lama2* myoblasts have differentiation process compromised at E17.5, contrasting to the E18.5 data suggesting, maybe through alternative pathways, that some recovery of myogenesis occurs. Alternatively, at E18.5, the slight increase in gene expression detected does not translate into functional proteins.

To try to understand what aspects of the myoblast differentiation pathways are altered by *Lama2*-deficiency, the Nfix pathway<sup>21</sup> was analyzed. The expression of *Nfix* and its target gene *Eno3* are slightly increased in E17.5 *dy<sup>W</sup>* epaxial muscle samples compared to WT (Figure 3.2A), however this is no longer the case at E18.5 (Figure 3.2B), which may indicate an attempt to recover from the upregulation at E17.5. Moreover, a significant increase in *Nfix* was observed in *Lama2* KO myoblast compared to WT (Figure 3.3C and D). This result goes in line with the recent studies of Rossi et al. where it was shown that dystrophic muscles typically feature cycles of degeneration, followed by attempts to regenerate the damage, and this dystrophic phenotype exacerbation is correlated with *Nfix* overexpression.<sup>28</sup>

Recent studies in *mdx* dystrophic mice, indicate that, during regeneration, *Nfix* directly regulates Myostatin, a negative regulator of skeletal muscle mass, controlling the temporal progression of the regeneration process.<sup>22</sup> However, our results on *Akirin1*, a target gene of Myostatin, expression levels did not detect any differences between WT and *dy<sup>W</sup>* epaxial muscle samples nor between *Lama2* KO C2C12 cells compared to WT (Figure 3.5A, B and C). Thus, further studies are necessary in the future, for example by measuring Myostatin levels directly both *in vivo* and in the C2C12 model. Myostatin has also been described to be a signalling molecule that inhibits proliferation of Pax7-expressing muscle precursors, and furthermore to down-regulated transcription factors that control proliferation and differentiation of embryonic muscle precursors, such as Pax-3, MyoD, Myf5, and Myogenin.<sup>58</sup> The results obtained showed a tendency for MyoD and a significant for Myf5 increase in *Lama2* KO C2C12 cells compared to WT (Figure 3.3C and 3.3D). Curiously, for Myf5 not only the protein levels were different between C2C12 WT and *Lama2* KO cells, but the cellular localization differed, with Myf5 being primarily localized in the nucleus in WT C2C12 cells and in the cytoplasm in *Lama2* KO cells (Figure 3.3B and B'). Is important to mention that MyoD levels showed a tendency to be increased in *Lama2* KO myoblasts compared to WT, further analysis of MyoD protein expression *in vivo* is necessary to validate this finding. Since MyoD and Myf5 are both MRF that will activate myogenin leading to myoblasts commitment, somehow it can compensate the Myf5 retention on cytoplasm. In a recent study, Panda et al. have also observed Myf5 localization both in the nucleus and in the cytoplasm in proliferating C2C12 myoblasts.<sup>59</sup> This may suggest that since Myf5 is a transcription factor that in its active form acts in the nucleus as an MRF, being retained in the cytoplasm indicates

that it is not activated, and consequently myoblast differentiation is compromised. These findings, together with the studies already reported about Nfix overexpression in muscular dystrophies<sup>28</sup> and how Nfix can regulate Myostatin expression<sup>22</sup> led to postulate the hypothesis schematically represented in Figure 4.1. Under this hypothesis it is suggested that Nfix overexpression in LAMA2-CMD can be a response to control Myostatin overexpression, due to *Lama2*-deficiency. Nfix overexpression will in turn lead to inhibition of Myostatin, that prevents Myf5 nuclear translocation in myoblasts, compromising Myogenin activation and consequently differentiation (Figure 4.1(1-3)). In the future it will be important to analyse the expression of Nfix, Myostatin, MyoD and Myf5 *in vivo* to further validate these findings.

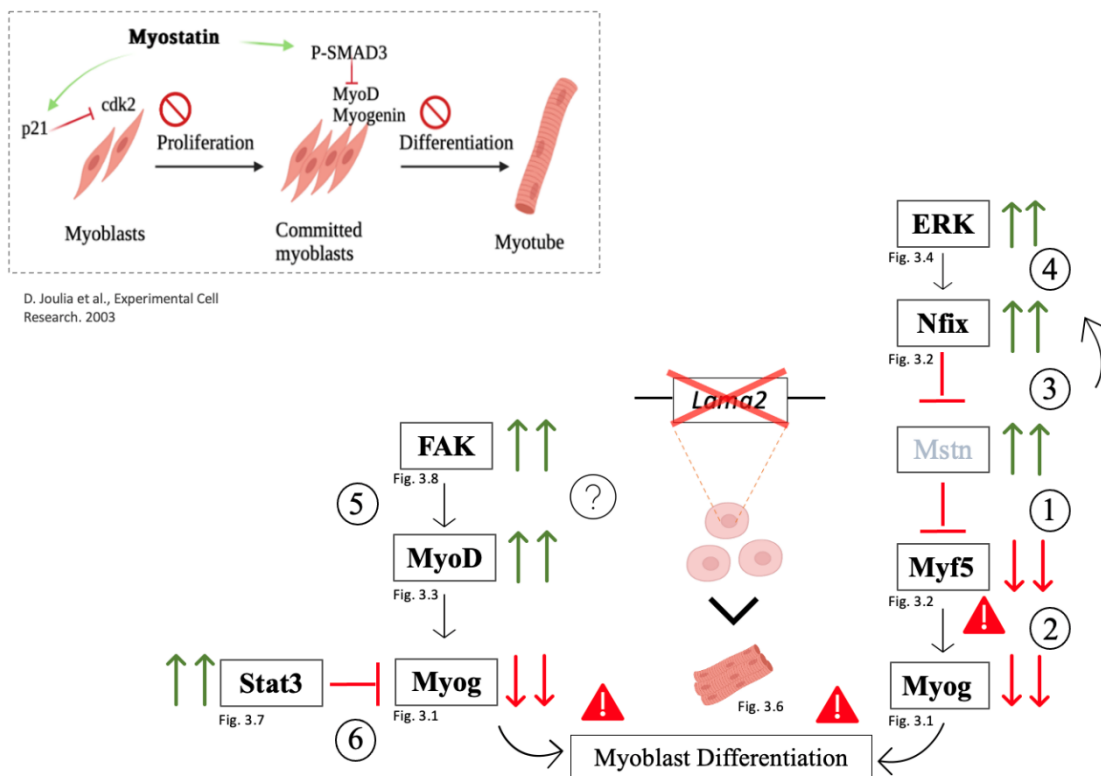


**Figure 4.1: Model for MuSCs/myoblasts differentiation defect in LAMA2-CMD.** MuSCs/myoblasts lacking *Lama2* lead to overexpression of Myostatin/Mstn (1), to control myoblasts proliferation and differentiation Mstn inhibits Myf5 (2) in MuSCs/myoblasts, consequently compromising Myog activation and therefore compromising differentiation (The main events upon myostatin activation are shown in the upper left side of the figure). The deregulation in differentiation and proliferation of myoblasts lead to Nfix overexpression (3), as a feedback mechanism to regulate Mstn expression and an attempt to promote MuSCs/myoblast differentiation. (4) The feedback response of overexpression of Nfix can be activated through ERK signaling, factor that is necessary for Nfix activation in fetal myoblasts. As an alternative pathway for MuSCs commitment (question mark indicate this hypothesis), when Myf5 is inhibited, FAK can activate MyoD expression (5) that will lead to the expression of Myogenin, allowing an alternative route to recover myoblasts differentiation. However, this attempt to progress towards differentiation is compromised by Stat3 pathway, since its overexpression is inhibiting myogenin expression (6). Green arrows indicate increased protein expression, Red arrows indicate decreased protein expression. Exclamation marks indicate signaling pathway and/or myoblast differentiation compromised.

Nfix expression during fetal development is controlled by JunB (a member of AP-1 family) activation, which in turn requires activation via ERK kinase that is repressed by the RhoA/Rock axis activity.<sup>26</sup>

P-Erk tends to be increased in C2C12 *Lama2* KO cells compared to WT (Figure 3.4B), which is in accordance with the increase of Nfix observed (Figure 3.2C).<sup>41</sup> The results obtained for P-Erk in C2C12 cells go in line with the ones described by Taglietti et al.<sup>27</sup>, where the increase of Erk signalling, regulated by RhoA/Rock signalling, leads to an increase in Nfix expression during the differentiation of foetal myoblasts<sup>27</sup> (Figure 4.1 (4)).

To further understand the link between Nfix and P-Erk in the context of *Lama2*-deficiency, it would be interesting to treat WT and *Lama2* KO C2C12 cells with an Erk inhibitor and assess if there are changes in Nfix expression. Since studies have reported that silencing Nfix ameliorates the dystrophic phenotype in *mdx* mice models<sup>28</sup>, the results obtained with these Erk inhibition experiment could highlight important pathways for therapeutic approaches in the future.

Another important factor in differentiation is Notch signalling, which was reported to inhibit myogenin and MyoD at fetal stages of development, promoting MuSCs self-renewal and inhibiting differentiation.<sup>53</sup> Also, in muscle regeneration after an injury, Notch signalling is downregulated allowing satellite cells to exit quiescence and enter the cell cycle, consequently activating MRF and further drive differentiation into myotubes.<sup>53</sup> The results obtained of *Notch1* expression, suggests a small tendency to be decreased in C2C12 *Lama2* KO myoblasts compared to WT (Figure 3.5A), and a tendency to be increased *in vivo* at E17.5 *dy*<sup>W</sup> epaxial muscle samples compared to WT (Figure 3.5B). However, the differences obtained were not significant and further analysis of Notch signalling is needed, for example by increasing the number of samples analysed by RT-qPCR, as well as analysing Notch protein levels in C2C12 cells and in fetal *dy*<sup>W</sup> muscle samples. The results obtained suggests that *Notch in vivo* at E17.5 play an important role in differentiation, since the increased expression observed known to be important for MuSCs proliferation, can be related to the compromised differentiation of myoblasts. Further analysis of Notch signaling and its target genes are necessary in the future to validate this findings.

As mentioned above, in skeletal muscle cells there is a basic range of Stat3 activity necessary to develop properly the skeletal muscle satellite cells<sup>35</sup> and *in vitro* studies demonstrated that deletion of *Stat3* leads to a reduction of MyoD and myogenin, and the same was observed *in vivo* causing impairment of post-traumatic muscle regeneration.<sup>36</sup> The host laboratory previously showed that P-Stat3 protein was increased in E17.5 muscles, suggesting that overactivation of Jak-Stat signalling is part of the mechanisms underlying the LAMA2-CMD onset and progression.<sup>20</sup> The results obtained in this project showed a significant increase of P-Stat3 in C2C12 *Lama2* KO cells compared to WT, as well as an increase *in vivo* in *dy*<sup>W</sup> epaxial muscles compared to WT at E17.5 (Figure 3.7A and B), in accordance with the previous findings. In contrast, in E18.5 *dy*<sup>W</sup> epaxial muscle samples compared to WT, there is a tendency for P-Stat3 to be decreased (Figure 3.7C), suggesting that at this time point there was a recovery, although not enough to restore the defect.

These findings indicate that in the absence of *Lama2* in C2C12 cells and in the context of LAMA2-CMD, P-Stat3 is significantly upregulated, which is concordant with one of Jak-Stat pathways mentioned before, where Stat3 can induce myoblasts proliferation, by the inhibition of Myogenin and consequently inhibit myoblasts differentiation (Figure 4.1 (6)).

As already mentioned, FAK has been described as an important factor for myoblast differentiation through MyoD activation and necessary for myotube formation.<sup>38</sup> The results obtained in this project showed a significant increase of P-FAK in *dy*<sup>W</sup> epaxial muscle samples compared to WT at E17.5 (Figure 3.8B), as well as a tendency in C2C12 *Lama2* KO cells compared to WT (Figure 3.8A). In contrast, there is a tendency for P-FAK to be decreased in *dy*<sup>W</sup> epaxial muscle samples at E18.5 compared to WT (Figure 3.8C), highlighting again the differences between E17.5 and E18.5. In addition, total FAK levels at E18.5 had a marked tendency to be increased (Figure 3.8C).

The decrease in P-FAK and the increase in total FAK at E18.5 in *dy<sup>W</sup>* epaxial muscle samples, suggest that myoblasts lacking *Lama2* lose the ability to activate FAK over time. It is known that upon activation by integrins, FAK undergoes autophosphorylation at Y397 and forms a complex with Src and other proteins that allow the trigger of downstream signaling.<sup>60</sup> The results obtained indicate that the presence of LN211/221 in the transition from E17.5 to E18.5 is essential, and the absence of these laminins and, consequently, of proper integrin binding to the basement membrane, somehow affects the activation of FAK. This, therefore, will prevent MyoD and myogenin activation and impair myoblast differentiation.<sup>61</sup> It will be important in the future to analyze protein expression levels of MyoD *in vivo* and further validate this hypothesis.

These results can point an alternative pathway for myoblast differentiation, since myogenin is being downregulated, cells can activate P-FAK and consequently the MRF MyoD that will activate myogenin expression, to compensate and promote differentiation in injured myofibers (Figure 4.1(5)).

In the future it would also be interesting to analyze the protein and gene expression levels of the mechanotransducer Yes-associated protein (Yap), since it has been reported that FAK controls the mechanical activation of Yap.<sup>62</sup> Yap is an important transcription regulator controlling, for example, the expression of Myf5<sup>63</sup> and this analysis will be important to further clarify the contribution of FAK pathway in myoblast differentiation.

Even though some differences between *in vivo* and *in vitro* models were observed in the current project, these may be explained by their different composition and characteristics. While *in vitro* experiments were performed using a monoculture of C2C12 cells, which lack cell diversity and the basement membrane niche, *in vivo*, the whole muscle, which includes MuSCs, myoblasts and myotubes were analyzed. Therefore, in this last model the communication between these different types of cells may lead to different responses and to compensatory mechanisms, that are not observed *in vitro*. Considering the overall results obtained in this project and the comparison between the results obtained *in vivo* and with C2C12 cells, they suggest that the *Lama2* C2C12 knockout cell line can be used as model for LAMA2-CMD, since in general, the analysis of gene and protein expressions performed had similar trends. Curiously, the analysis obtained with C2C12 *in vitro* model resembles more the results obtained *in vivo* at E17.5, as shown for the gene expression levels of *Myog* and *Myf1* and protein levels of P-Stat3 and P-FAK. These findings suggest that this *in vitro* model resembles an earlier period of MuSCs and myoblasts, which is important since the fetal stage of development is the one of interest for this project. Therefore, this project also represents an important step forward, in order to replace *in vivo* and *ex vivo* models for MuSCs, where MuSCs collection and isolation process from mice proves to be complex, time-consuming and implicates the use of a high number of animals.

As a last goal, this project aimed at analyzing if the pathways altered in LAMA2-CMD myoblasts were also altered in *LAMA2* deficient cancer cell lines.<sup>43</sup> As mentioned before, laminins are one of the most predominant glycoprotein families in ECM and their structural and functional importance is well established. Not surprisingly, it has been shown that these proteins are heavily involved in tumour angiogenesis, cell invasion, metastasis development and drug resistance.<sup>44</sup> In this project *LAMA2* KO cell lines of melanoma and colorectal cancer cells, which were previously established by members of the host laboratory, were used to investigate signalling pathways implicated in differentiation. Analysis of the *LAMA2*-deficient cell lines showed a tendency for a decrease in the expression of *ENO1* in melanoma cancer cell line, while in the colorectal cancer cell lines no differences were observed (Figure 3.9B, C). According to recent studies, ENO1 has significantly higher expression in melanoma cell lines in comparison to normal melanocytes<sup>64</sup> and overexpression of ENO1 in colorectal (HCT116) cancer cell lines promoted cell proliferation, migration, and invasion *in vitro* as well as tumorigenesis and metastasis *in vivo*<sup>65</sup>. Considering the reduction in *ENO1* upon *LAMA2* deletion in melanoma cells, this may suggest that there is a reduction in proliferation and migration. Further analysis should be performed to test this hypothesis.

The NOTCH signalling pathway and its modulators are directly related to growth, verticalization and metastasis in melanoma<sup>66</sup> and overexpression of *NOTCH1* has been shown to initiate and



being responsible for colorectal cancer proliferation.<sup>67</sup> The results obtained demonstrate that in the absence of *LAMA2* in melanoma cancer cell lines *NOTCH1* expression is not affected (Figure 3.9 B), contrasting to the results in the colorectal cancer cell lines where there is a tendency towards an increase (Figure 3.9 C).

As already mentioned before, Stat3 is a key element in skeletal muscle cells and the results obtained showed that in the absence of *Lama2* P-Stat3 is overexpressed in myoblasts (Figure 3.7A), as previously observed by the host laboratory.<sup>20</sup> It has been reported that STAT3 is a critical transcription factor that has been firmly associated with colorectal cancer initiation and development.<sup>68</sup> The data obtained revealed that in the absence of *LAMA2*, P-STAT3 has a marked tendency to be increased in the colorectal single cell KO compared to WT (Figure 3.9 D), together indicating that *LAMA2*-deficiency contributes to colorectal cancer development. This also suggests that besides the type of cell or disease model analysed, the absence of laminin 211/221 in ECM leads to an overactivation of P-STAT3, i.e., P-STAT3 responds to the loss of an important component of ECM.

The results obtained in this project showed that *Lama2*-deficiency leads to an increase of Nfix expression in the context of LAMA2-CMD. Although recent studies suggests that Nfix contributes to prostatic hyperplasia, by regulating prostate specific gene expression, and as a tumour-suppressor gene in colorectal cancer and squamous cell carcinoma<sup>25</sup>, the results obtained did not show differences in NFIX expression in melanoma *LAMA2* KO cancer cell lines compared to WT. These indicates that *LAMA2* absence did not affect NFIX expression in melanoma cancer cell lines (Figure 3.9 A) and this relationship may only be relevant during muscle development. The impact of *LAMA2* deletion in cancer will need further analysis to co-substantiate the results found in this project.

Overall, this project highlights how *Lama2*-deficiency affects several important pathways that will impact myoblasts differentiation *in vivo* and in the C2C12 cell model which are important to understand the onset of the disease. It also establishes the C2C12 myogenic cell line as a relevant *in vitro* model for LAMA2-CMD, which allows to better understand the pathways affected in the disease. In addition, this project initiates the study of the impact of *LAMA2*-deficiency in cancer cell lines. Identifying these pathways, and the mechanism by which they act, is essential for the development of therapies that target disease onset directly.

## Annex

**Table S1 PCR protocol for mouse genotyping.**

Cycles			
Step #	Temp °C	Time	
1	94	2 min	
2	94	20 sec	
3	65	15 sec	-0,5°C per cycle decrease
4	68	10 sec	
5			Repeat steps 2-4 for 10 cycles
(Touchdown)			
6	94	15 sec	
7	60	15 sec	
8	72	10 sec	
9			Repeat steps 6-8 for 28 cycles
10	72	2 min	
11	12		Hold

**Table S2 List of primers used for genotyping.**

	Primer	Sequence
<i>dy<sup>W</sup></i>	Primer 1	5' ACTGCCCTTTC TCACCCACCCTT 3'
	Primer 2	5' GTTGATGCGCTTGGGACTG 3'
	Primer 3	5' GTCGACGACGACAGTACTGGCCTCAG 3'

**Table S3 List of primers used in Real-Time qPCR analyses**

Gene	Animal	Primer	Sequence
<i>Arbp0</i>	Mouse	Forward	5' CTTTGGGCATCACCACGAA 3'
		Reverse	5' GCTGGCTCCCACCTTGTCT 3'
<i>Lama2</i>	Mouse	Forward	5' TGAAAGCAAGGCCAGAAGTCA 3'
		Reverse	5' ACAAACCAGGCTTGGGGAA 3'
<i>Pax7</i>	Mouse	Forward	5' ATCAAGCCAGGAGACAGCTTGC 3'
		Reverse	5' TGTGTGGACAGGCTCACGTTTT 3'
<i>Nfix</i>	Mouse	Forward	5' TTCATTCAACAACGACAGGCGCC 3'
		Reverse	5' AACCAGGACTGAGACTGCTGTG 3'
<i>Eno3</i>	Mouse	Forward	5' TACCGCAACGGCAAGTATGA 3'
		Reverse	5' CTCAATGGAGACCACGGGAT 3'
<i>Ckm</i>	Mouse	Forward	5' GGTGGACAACCCAGGTCAC 3'
		Reverse	5' CATAGTTGGGGTCCAGGTCG 3'
<i>Myog</i>	Mouse	Forward	5' GTCCAACCCAGGAGATCAT 3'
		Reverse	5' CCACGATGGACGTAAGGGAG 3'
<i>Tubb6</i>	Mouse	Forward	5' AAGAAGTACGTACCCAGGGC 3'
		Reverse	5' CACCCGTCTGTCCGAAGAT 3'
<i>Myl1</i>	Mouse	Forward	5' CGGAGTTTTCAAGCACGCAA 3'
		Reverse	5' TCTGCATGGTGGTAAGCTGG 3'
<i>Notch1</i>	Mouse	Forward	5' CAACTGCCAGAACCTTGTGC 3'
		Reverse	5' AGAGTGACGTCAATGCCTCG 3'
<i>Mighty</i>	Mouse	Forward	5' ATCATGCGGCGATACGGGACA 3'
		Reverse	5' AGTGTACAGCAGCCATCTCTTGA 3'
<i>Itga7</i>	Mouse	Forward	5' CCGGCTATCGCCTTCAATCT 3'
		Reverse	5' CCACCAGCAGCCAGCTC 3'
<i>LAMA2</i>	Human	Forward	5' TGAAAGCAAGGCCAGAAGTCA 3'
		Reverse	5' ACAAACCAGGCTTGGGGAA 3'
<i>ENO1</i>	Human	Forward	5' TCTCTTCACTCAAAGGTCTCT 3'
		Reverse	5' CCATGGGCTGTGGGTTCTAA 3'
<i>NOTCH1</i>	Human	Forward	5' GACATGCCACGTGGTGGGA 3'
		Reverse	5' GGCACGATTTCCCTGACCA 3'
<i>ACTB</i>	Human	Forward	5' GAGCACAGAGCCTCGCCTT 3'
		Reverse	5' TCATCATCCATGGTGAGCTGG 3'

**Table S4 Real-Time PCR protocol used in CFX96™**

Real-Time PCR System		Bio-Rad CFX96™
Setting/Mode		SYBR only
Polymerase Activation and DNA Denaturation		30 sec at 95°C
Amplification	Denaturation at 95°C	5 sec
	Annealing/Extension and Plate Read at 60°C	15sec
	Cycles	40
Melting Curve Analysis		65-95°C 0.5°C increments at 5 sec/step

**Table S5 Antibodies and dilutions used for Western Blot and Immunofluorescence**

	<b>Antibody</b>	<b>Raised in</b>	<b>Primary vs Secondary</b>	<b>Dilution</b>	<b>Catalog number</b>	<b>Brand</b>
<b>Western Blot</b>	Histone H3	Rabbit	Primary	1:2000	9715	Cell Signaling
	Vinculin	Mouse	Primary	1:1000	ab18058	Abcam
	P-ERK	Mouse	Primary	1:1000	sc-7383	Santa Cruz
	ERK	Rabbit	Primary	1:1000	137F5	Cell Signaling
	STAT3	Rabbit	Primary	1:1000	12640	Cell Signaling
	P-STAT3 T705	Rabbit	Primary	1:1000	9145	Cell Signaling
	FAK	Mouse	Primary	1:1000	sc-1688	Santa Cruz
	P-FAK Tyr397	Rabbit	Primary	1:1000	PA5-17084	Invitrogen
	MyoD	Mouse	Primary	1:1000	MA5-12902	FisherScientific
	GAPDH	Rabbit	Primary	1:1000	2118	Cell Signaling
	Anti-Mouse IgG-HRP	Goat	Secondary	1:5000	AB_10015289	Jackson Immunoresearch Europe
Anti-Rabbit IgG-HRP	Goat	Secondary	1:5000	AB_2313567	Jackson Immunoresearch Europe	
<b>Immunofluorescence</b>	Nfix	Rabbit	Primary	1:200	NBP2-15039	Novus
	Pax7	Mouse	Primary	1:50	Pax7-c	DSHB
	Myf5	Mouse	Primary	1:150	Sc-302	Santa Cruz
	Myosin heavy chain	Mouse	Primary	1:100	MF-20	DSHB
	Fibronectin	Rabbit	Primary	1:200	F3648-2ML	Sigma
	Alexa Fluor 488 Anti-Rabbit IgG	Goat	Secondary	1:500	A11070	Invitrogen
	Alexa Fluor 568 Anti-Mouse IgG	Goat	Secondary	1:500	A11019	Invitrogen

## Bibliography

1. Frantz, C., Stewart, K. M. & Weaver, V. M. The extracellular matrix at a glance. *J Cell Sci* **123**, 4195 (2010).
2. Hastings, J. F., Skhinas, J. N., Fey, D., Croucher, D. R. & Cox, T. R. The extracellular matrix as a key regulator of intracellular signalling networks. *Br J Pharmacol* **176**, 82–92 (2019).
3. Lu, P., Takai, K., Weaver, V. M. & Werb, Z. Extracellular Matrix Degradation and Remodeling in Development and Disease. *Cold Spring Harb Perspect Biol* **3**, (2011).
4. Martins, S. G., Zilhão, R., Thorsteinsdóttir, S. & Carlos, A. R. Linking Oxidative Stress and DNA Damage to Changes in the Expression of Extracellular Matrix Components. *Front Genet* **12**, 1279 (2021).
5. Thorsteinsdóttir, S., Deries, M., Cachaço, A. S. & Bajanca, F. The extracellular matrix dimension of skeletal muscle development. *Dev Biol* **354**, 191–207 (2011).
6. Rozario, T. & DeSimone, D. W. The extracellular matrix in development and morphogenesis: A dynamic view. *Dev Biol* **341**, 126–140 (2010).
7. Sekiguchi, R. & Yamada, K. M. Basement membranes in development and disease. *Curr Top Dev Biol* **130**, 143 (2018).
8. Yurchenco, P. D., Amenta, P. S. & Patton, B. L. Basement membrane assembly, stability and activities observed through a developmental lens. *Matrix Biology* **22**, 521–538 (2004).
9. Yue, B. Biology of the extracellular matrix: An overview. *Journal of Glaucoma* vol. 23 S20–S23 Preprint at <https://doi.org/10.1097/IJG.000000000000108> (2014).
10. Barraza-Flores, P., Bates, C. R., Oliveira-Santos, A. & Burkin, D. J. Laminin and Integrin in LAMA2-Related Congenital Muscular Dystrophy: From Disease to Therapeutics. *Frontiers in Molecular Neuroscience* vol. 13 Preprint at <https://doi.org/10.3389/fnmol.2020.00001> (2020).
11. Rasmussen, D. G. K. & Karsdal, M. A. Laminins. in *Biochemistry of Collagens, Laminins and Elastin: Structure, Function and Biomarkers* 209–263 (Elsevier, 2019). doi:10.1016/B978-0-12-817068-7.00029-X.
12. Hohenester, E. & Yurchenco, P. D. Laminins in basement membrane assembly. <http://dx.doi.org/10.4161/cam.21831> **7**, 56–63 (2012).
13. Barraza-Flores, P. *et al.* Human laminin-111 and laminin-211 protein therapy prevents muscle disease progression in an immunodeficient mouse model of LAMA2-CMD. *Skelet Muscle* **10**, (2020).
14. Oliveira, J. *et al.* LAMA2 gene mutation update: Toward a more comprehensive picture of the laminin- $\alpha$ 2 variome and its related phenotypes. *Hum Mutat* **39**, 1314–1337 (2018).
15. Yurchenco, P. D., McKee, K. K., Reinhard, J. R. & Rüegg, M. A. Laminin-deficient muscular dystrophy: Molecular pathogenesis and structural repair strategies. *Matrix Biology* vols 71–72 174–187 Preprint at <https://doi.org/10.1016/j.matbio.2017.11.009> (2018).
16. Chal, J. & Pourquié, O. Making muscle: skeletal myogenesis in vivo and in vitro. *Development* **144**, 2104–2122 (2017).
17. Rossi, G. & Messina, G. Comparative myogenesis in teleosts and mammals. *Cellular and Molecular Life Sciences* vol. 71 3081–3099 Preprint at <https://doi.org/10.1007/s00018-014-1604-5> (2014).
18. Deries, M. & Thorsteinsdóttir, S. Axial and limb muscle development: dialogue with the neighbourhood. *Cellular and Molecular Life Sciences* vol. 73 4415–4431 Preprint at <https://doi.org/10.1007/s00018-016-2298-7> (2016).
19. Venters, S. J., Thorsteinsdóttir, S. & Duxson, M. J. Early Development of the Myotome in the Mouse. *Developmental Dynamics* (1999) doi:10.1002/(SICI)1097-0177(199911)216:3.
20. Nunes, A. M. *et al.* Impaired fetal muscle development and JAK-STAT activation mark disease onset and progression in a mouse model for merosin-deficient congenital muscular dystrophy. *Hum Mol Genet* **26**, 2018–2033 (2017).

21. Deries, M., Gonçalves, A. B. & Thorsteinsdóttir, S. *Skeletal muscle development-from stem cells to body movement Springer Learning Series: 'Concepts and Applications of Stem Cell Biology: a Guide for Students'*. (\*equal contribution).
22. Rossi, G. *et al.* Nfix Regulates Temporal Progression of Muscle Regeneration through Modulation of Myostatin Expression. *Cell Rep* **14**, 2238 (2016).
23. Gronostajski, R. M. *Roles of the NFI/CTF gene family in transcription and development. Gene* vol. 249 [www.elsevier.com/locate/gene](http://www.elsevier.com/locate/gene) (2000).
24. Gronostajski, R., Chaudhry, A. Z., Lyons, G. E. & Gronostajski, R. M. *Expression patterns of the four nuclear factor I genes during mouse embryogenesis indicate a potential role in d... Expression Patterns of the Four Nuclear Factor I Genes During Mouse Embryogenesis Indicate a Potential Role in Development. Dev. Dyn* vol. 208 (1997).
25. Piper, M., Gronostajski, R. & Messina, G. Nuclear Factor One X in Development and Disease. *Trends in Cell Biology* vol. 29 20–30 Preprint at <https://doi.org/10.1016/j.tcb.2018.09.003> (2019).
26. Taglietti, V. *et al.* Rhoa and erk signalling regulate the expression of the transcription factor nfix in myogenic cells. *Development (Cambridge)* **145**, (2018).
27. Messina, G. *et al.* Nfix Regulates Fetal-Specific Transcription in Developing Skeletal Muscle. *Cell* **140**, 554–566 (2010).
28. Rossi, G. *et al.* Silencing Nfix rescues muscular dystrophy by delaying muscle regeneration. *Nat Commun* **8**, (2017).
29. Grabowska, M. M. *et al.* NFI transcription factors interact with FOXA1 to regulate prostate-specific gene expression. *Molecular Endocrinology* **28**, 949–964 (2014).
30. Rahman, N. I. A., Abdul Murad, N. A., Mollah, M. M., Jamal, R. & Harun, R. NFIX as a Master Regulator for Lung Cancer Progression. *Front Pharmacol* **8**, (2017).
31. Schuelke, M. *et al.* Myostatin Mutation Associated with Gross Muscle Hypertrophy in a Child. <https://doi.org/10.1056/NEJMoa040933> **350**, 2682–2688 (2004).
32. Bernardi, H. *et al.* Mechanisms Involved in the Inhibition of Myoblast Proliferation and Differentiation by Myostatin Autophagy, mitochondrial remodeling and exercise View project Mechanisms involved in the inhibition of myoblast proliferation and differentiation by myostatin. (2003) doi:10.1016/S0014-4827(03)00074-0.
33. Renshaw, B., Getting, D. & Mackenzie, S. The Central Role of Myostatin in Skeletal Muscle and Whole Body Homeostasis. *Acta Physiologica* **205**, 324–364 (2012).
34. Diao, Y., Wang, X. & Wu, Z. SOCS1, SOCS3, and PIAS1 Promote Myogenic Differentiation by Inhibiting the Leukemia Inhibitory Factor-Induced JAK1/STAT1/STAT3 Pathway. *Mol Cell Biol* **29**, 5084–5093 (2009).
35. Jaśkiewicz, A., Domoradzki, T. & Pajak, B. Targeting the JAK2/STAT3 pathway—can we compare it to the two faces of the god janus? *International Journal of Molecular Sciences* vol. 21 1–17 Preprint at <https://doi.org/10.3390/ijms21218261> (2020).
36. Tierney, M. T. *et al.* STAT3 signaling controls satellite cell expansion and skeletal muscle repair. *Nat Med* **20**, 1182–1186 (2014).
37. Mitra, S. K., Hanson, D. A. & Schlaepfer, D. D. Focal adhesion kinase: in command and control of cell motility. *Nature Reviews Molecular Cell Biology* 2005 6:1 **6**, 56–68 (2005).
38. Graham, Z. A., Gallagher, P. M. & Cardozo, C. P. Focal adhesion kinase and its role in skeletal muscle. *J Muscle Res Cell Motil* **36**, 305 (2015).
39. Han, J. W., Lee, H. J., Bae, G. U. & Kang, J. S. Promyogenic function of Integrin/FAK signaling is mediated by Cdc42 and MyoD. *Cell Signal* **23**, 1162–1169 (2011).
40. Kanagawa, M. & Toda, T. The genetic and molecular basis of muscular dystrophy: roles of cell–matrix linkage in the pathogenesis. *Journal of Human Genetics* 2006 51:11 **51**, 915–926 (2006).
41. Durbeej, M. Laminin- $\alpha$ 2 Chain-Deficient Congenital Muscular Dystrophy. Pathophysiology and Development of Treatment. *Curr Top Membr* **76**, 31–60 (2015).

42. Saclier, M., Temponi, G., Bonfanti, C. & Messina, G. Selective ablation of Nfix in Macrophages preserves Muscular Dystrophy by inhibiting FAPs-dependent fibrosis. *bioRxiv* 2021.05.12.443809 (2021) doi:10.1101/2021.05.12.443809.
43. Fang, M., Yuan, J., Peng, C. & Li, Y. Collagen as a double-edged sword in tumor progression. *Tumour Biol* **35**, 2871–2882 (2014).
44. Qin, Y., Rodin, S., Simonson, O. E. & Hollande, F. Laminins and cancer stem cells: Partners in crime? *Seminars in Cancer Biology* vol. 45 3–12 Preprint at <https://doi.org/10.1016/j.semcancer.2016.07.004> (2017).
45. Qiu, T. *et al.* Identification of genes associated with melanoma metastasis. *Kaohsiung J Med Sci* **31**, 553–561 (2015).
46. Liang, J. *et al.* Mex3a interacts with LAMA2 to promote lung adenocarcinoma metastasis via PI3K/AKT pathway. *Cell Death & Disease* **2020 11:8 11**, 1–15 (2020).
47. Ge, J. *et al.* NFIX downregulation independently predicts poor prognosis in lung adenocarcinoma, but not in squamous cell carcinoma. *Future Oncology* **14**, 3135–3144 (2018).
48. Thomas, S. J., Snowden, J. A., Zeidler, M. P. & Danson, S. J. The role of JAK/STAT signalling in the pathogenesis, prognosis and treatment of solid tumours. *British Journal of Cancer* **2015 113:3 113**, 365–371 (2015).
49. Murphy, M. & Kardon, G. *Origin of vertebrate limb muscle: The role of progenitor and myoblast populations. Current Topics in Developmental Biology* vol. 96 (NIH Public Access, 2011).
50. Yurchenco, P. D., McKee, K. K., Reinhard, J. R. & Rüegg, M. A. Laminin-deficient Muscular Dystrophy: Molecular Pathogenesis and Structural Repair Strategies. *Matrix Biol* **71–72**, 174 (2018).
51. Burattini S *et al.* C2C12 murine myoblasts as a model of skeletal muscle development: Morpho-functional characterization. [https://www.researchgate.net/publication/8134286\\_C2C12\\_murine\\_myoblasts\\_as\\_a\\_model\\_of\\_skeletal\\_muscle\\_development\\_Morpho-functional\\_characterization](https://www.researchgate.net/publication/8134286_C2C12_murine_myoblasts_as_a_model_of_skeletal_muscle_development_Morpho-functional_characterization) (2004).
52. Melo, C. E. M. de & Carlos, A. R. C. M. The impact of Lama2-deficiency on cell cycle regulation and survival. *Repositório da Universidade de Lisboa* <https://repositorio.ul.pt/handle/10451/53636> (2022).
53. Koch, U., Lehal, R. & Radtke, F. Stem cells living with a Notch. *Development* **140**, 689–704 (2013).
54. Walker, C., Mojares, E. & del Río Hernández, A. Role of Extracellular Matrix in Development and Cancer Progression. *Int J Mol Sci* **19**, (2018).
55. Lee, S. *et al.* Identification of GABRA1 and LAMA2 as new DNA methylation markers in colorectal cancer. *Int J Oncol* **40**, 889–898 (2012).
56. Huang, C. K., Sun, Y., Lv, L. & Ping, Y. ENO1 and Cancer. *Mol Ther Oncolytics* **24**, 288–298 (2022).
57. Lobry, C., Oh, P., Mansour, M. R., Thomas Look, A. & Aifantis, I. Notch signaling: switching an oncogene to a tumor suppressor. *Blood* **123**, 2451–2459 (2014).
58. Amthor, H., Otto, A., Macharia, R., McKinnell, I. & Patel, K. Myostatin imposes reversible quiescence on embryonic muscle precursors. *Developmental Dynamics* **235**, 672–680 (2006).
59. Panda, A. C. *et al.* Novel RNA-binding activity of MYF5 enhances Ccnd1/Cyclin D1 mRNA translation during myogenesis. *Nucleic Acids Res* **44**, 2393 (2016).
60. Guan, J. L. Integrin signaling through FAK in the regulation of mammary stem cells and breast cancer. *IUBMB Life* **62**, 268–276 (2010).
61. Han, J. W., Lee, H. J., Bae, G. U. & Kang, J. S. Promyogenic function of Integrin/FAK signaling is mediated by Cdo, Cdc42 and MyoD. *Cell Signal* **23**, 1162–1169 (2011).
62. Lachowski, D. *et al.* FAK controls the mechanical activation of YAP, a transcriptional regulator required for durotaxis. *The FASEB Journal* (2018) doi:10.1096/fj.201700721R.
63. Fischer, M., Rikeit, P., Knaus, P. & Coirault, C. YAP-mediated mechanotransduction in skeletal muscle. *Front Physiol* **7**, 41 (2016).

64. Hippner, M. *et al.* Alpha-Enolase (ENO1) Correlates with Invasiveness of Cutaneous Melanoma—An In Vitro and a Clinical Study. *Diagnostics* 2022, Vol. 12, Page 254 **12**, 254 (2022).
65. Zhan, P. *et al.*  $\alpha$ -enolase promotes tumorigenesis and metastasis via regulating AMPK/mTOR pathway in colorectal cancer. *Mol Carcinog* **56**, 1427–1437 (2017).
66. Dal, L. *et al.* Identification and quantification of notch receptors in human cutaneous melanoma using molecular biology techniques: literature review. *Surgical and Experimental Pathology* 2020 3:1 **3**, 1–9 (2020).
67. Tyagi, A., Sharma, A. K. & Damodaran, C. A Review on Notch Signaling and Colorectal Cancer. *Cells* **9**, (2020).
68. Gargalionis, A. N., Papavassiliou, K. A. & Papavassiliou, A. G. Targeting STAT3 Signaling Pathway in Colorectal Cancer. *Biomedicines* **9**, (2021).